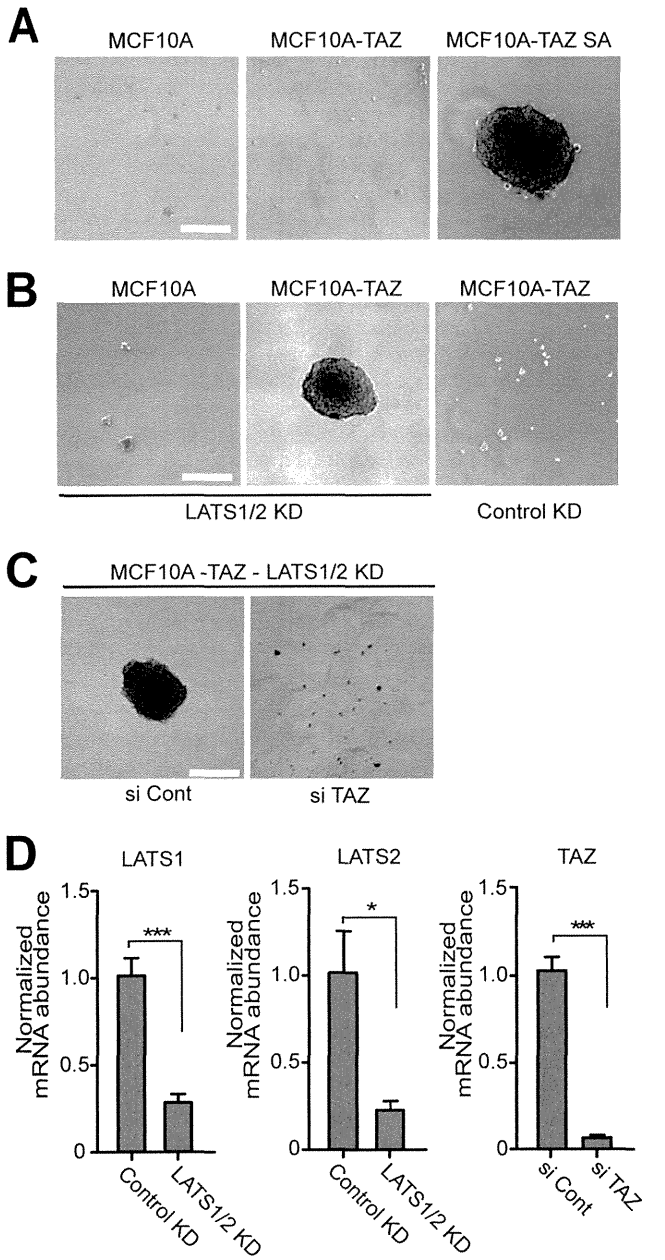

FIG 1 MCF10A cells form mammospheres depending on TAZ activity. (A) Parent MCF10A cells, TAZ-expressing MCF10A cells (MCF10A-TAZ), and TAZ SA-expressing MCF10A cells (MCF10A-TAZ SA) were cultured under mammosphere-forming conditions. Only MCF10A-TAZ SA formed spheres. (B) LATS1 and LATS2 were knocked down in parent MCF10A and MCF10A-TAZ cells. LATS1 and LATS2 knockdown (KD) provided MCF10A-TAZ cells with the capacity to form mammospheres. Parent MCF10A cells could not form mammospheres even with LATS1 and LATS2 knockdown. (C) Additional knockdown of TAZ in MCF10A-TAZ cells with LATS1 and LATS2 knockdown abolished the mammosphere formation induced by LATS1 and LATS2 knockdown. si Cont, control dsRNA; si TAZ, TAZ dsRNA. Bars, 200 μm. (D) Validation of LATS1, LATS2, and TAZ knockdowns in MCF10A cells. Data are means and standard errors of the means. *, $P < 0.05$; ***, $P < 0.001$.

compound named IBS008738, which showed the most significant effect (Fig. 2A). IBC008738 facilitated myogenesis and enhanced MHC expression (Fig. 2B). The effect was also detectable at 1 μM (Fig. 2C).

IBS008738 enhances protein expression of myogenic differentiation, and its effect depends on TAZ. When C2C12 cells were cultured with IBS008738 under growth conditions for 24 h and transferred to differentiation conditions, MyoD expression was slightly higher at 0 h (Fig. 2D). This finding suggests that IBS008738 has some ability, if not a significant one, to promote MyoD expression under growth conditions. MyoD expression more clearly increased at 24 and 48 h and declined at 72 h. Myogenin became detectable at 24 h in both control and IBS008738-treated cells, and IBS008738 increased its expression. An MHC signal started to be visible at 24 h in IBS008738-treated cells and was more apparent at 48 and 72 h than in control cells. IBS008738 also enhanced TAZ expression, with a peak at 24 h. It slightly facilitated the decrease in Pax7 but had no effect on Pax3. We knocked down endogenous TAZ with a dsRNA or shRNA retrovirus vector and confirmed that TAZ knockdown abolished the effect of IBS008738 (Fig. 2E and F).

IBS008738 enhances mRNAs of myogenic markers but not of myofusion markers. In a quantitative real-time PCR assay, the levels of transcription of the genes for myogenin and MyoD at 24 h under differentiation conditions were higher in IBS008738-treated cells but the differences were no more significant at 72 h (Fig. 3A). In contrast to TAZ protein expression, TAZ gene expression was not changed at 24 h and was reduced at 72 h. We tested the effect of IBS008738 on the expression of the genes that are regarded as TAZ targets in epithelial cells. The connective tissue growth factor (CTGF)- and cyclin D1-encoding genes were not increased in C2C12 cells by IBS008738 treatment (Fig. 3A). IBS008738 did not enhance but rather suppressed the genes for myofusion markers, including M-cadherin, calpain 1, and caveolin 3, which suggests that the enhanced myofusion observed in IBS008738-treated C2C12 cells reflects the facilitation of myogenesis at an early stage and is not directly driven by an enhanced fusion process (Fig. 3A).

IBS008738 enhances the MyoD-responsive myogenin promoter reporter in C2C12 cells. We tested whether and how IBS008738 affects the reporter activities regulated by various TAZ-interacting transcriptional factors in C2C12 cells. We exogenously expressed each reporter and TAZ in C2C12 cells and treated them with DMSO or IBS008738. TAZ overexpression enhanced the activities of all reporters, including the MyoD, TEAD, SMAD, and Pax3 reporters (Fig. 3B, first and the second columns). IBS008738 further enhanced only the MyoD reporter in C2C12 cells (Fig. 3B, second and third columns). In contrast to the result in HEK293 cells, IBS008738 did not enhance TEAD reporter activity in C2C12 cells. It did not enhance the effect of TAZ on the SMAD or Pax3 reporter either.

IBS008738 increases the association of MyoD with the myogenin promoter. MyoD, TEAD4, and Pax3 were immunoprecipitated from differentiated C2C12 cells treated with the control DMSO or IBS008738, and ChIP assays were performed. IBS008738 enhanced MyoD binding to the myogenin promoter but had no effect on the association of TEAD4 with the CTGF promoter (Fig. 3C). IBS008738 reduced the binding of Pax3 to the Myf5 promoter (Fig. 3C).

IBS008738 enhances the interaction of TAZ and MyoD. We tested the effect of IBS008738 on the interaction between TAZ and MyoD by immunoprecipitating endogenous TAZ from C2C12 cells. When MyoD was immunoprecipitated from C2C12 cells, IBS008738 slightly increased the amount of TAZ coimmunoprecipitated (Fig. 4A). However, as IBS008738 increased the expres-

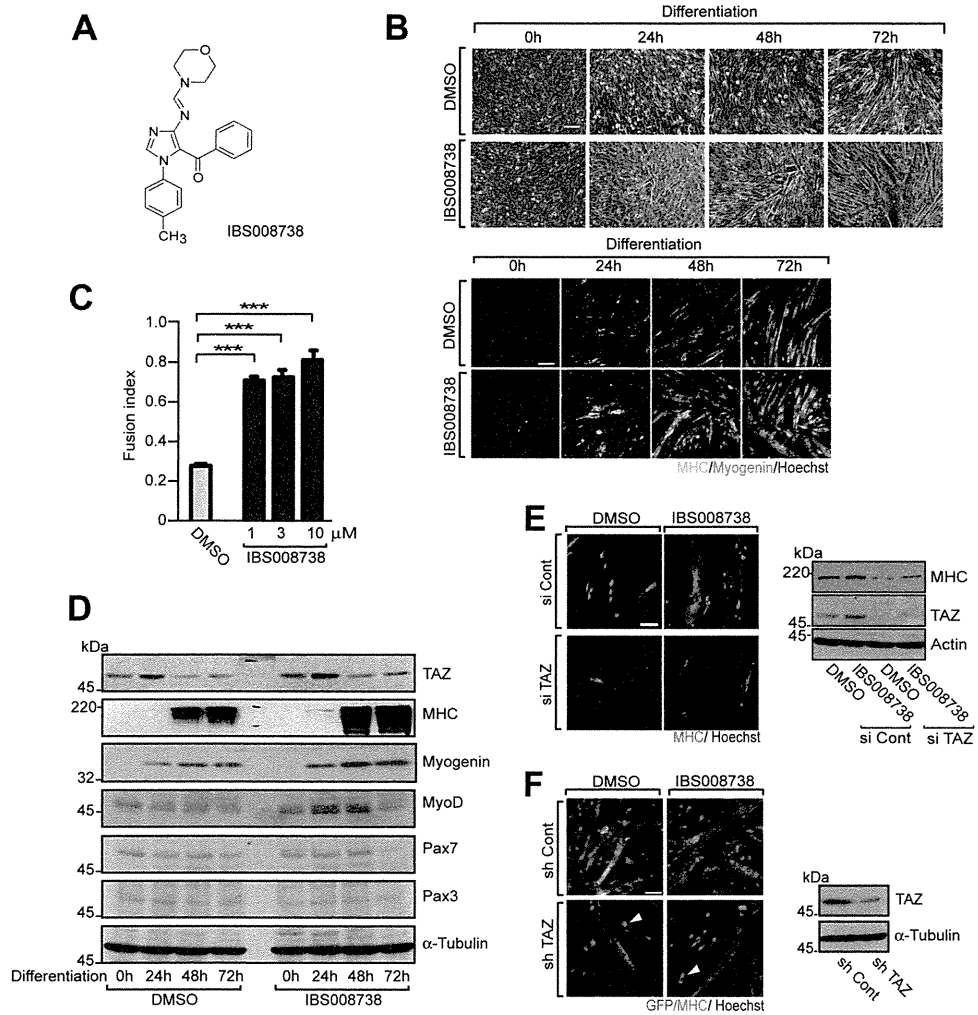

FIG 2 The TAZ activator candidate compound IBS008738 facilitates C2C12 myogenesis. (A) Chemical structure of IBS008738. (B) Phase-contrast images and immunofluorescence assays of C2C12 cells treated with DMSO or IBS008738. IBS008738 at 10 μM was added after the cells were switched to differentiation conditions. Cells were fixed at the time points indicated and immunostained with anti-MHC (green) and antimyogenin (red) antibodies (lower panels). Nuclei were visualized with Hoechst 33342. Bars, 100 μm. (C) C2C12 cells were treated with various doses of IBS008738. Myogenesis was evaluated by determining the myofusion index at 72 h. Data are means and standard errors of the means. ***, $P < 0.001$. (D) C2C12 cells were treated with DMSO or IBS008738 under growth conditions for 24 h, switched to differentiation conditions, and cultured for the indicated time periods with IBS008738 under differentiation conditions. The cells were harvested immediately after culture under growth conditions (0 h) or after 24, 48, or 72 h of culture under differentiation conditions. The lysates were immunoblotted with the antibodies indicated. α-Tubulin was used as the loading control. (E) C2C12 cells were transfected with control dsRNA (si Cont) or TAZ dsRNA (si TAZ). The cells were treated with DMSO or IBS008738 and fixed at 72 h under differentiation conditions. MHC was immunostained (red). The lysates were immunoblotted with anti-MHC and anti-TAZ antibodies. TAZ knockdown suppressed MHC expression in cells treated with DMSO (lane 3). TAZ knockdown abolished the effect of IBS008738 (lane 4). Immunoblotting with anti-TAZ antibody demonstrates that TAZ was efficiently knocked down. Bars, 100 μm. (F) Endogenous TAZ was suppressed by using shRNA in DMSO- and IBS008738-treated C2C12 cells. The retrovirus shRNA vectors harbor GFP as a tracer. MHC (red) expression is reduced in cells transfected with TAZ shRNA (green, arrowheads). The panel on the right shows the validation of shRNA.

sion of endogenous MyoD, the amount of MyoD immunoprecipitated itself increased. To circumvent this issue, we expressed FLAG-TAZ and HA-MyoD in HEK293 cells and performed immunoprecipitation with anti-FLAG M2 affinity gel. Under IBS008738 treatment, the interaction of HA-MyoD with FLAG-TAZ was enhanced (Fig. 4B, arrowhead). In the immunofluorescence of C2C12 cells, both endogenous MyoD and TAZ were diffusely distributed in the nucleus under growth conditions but formed dots under differentiation conditions (Fig. 4C, DMSO, top and middle). Interestingly, the expression of TAZ and MyoD was not the same in all of the cells. Some cells strongly expressed TAZ (red), whereas other cells expressed more MyoD (green) at 24 h after differentiation (Fig. 4C, middle). This finding is reminiscent of the previously reported heterogeneity of Myf5 expression and may suggest that MyoD and TAZ expression fluctuates like that of Myf5 in C2C12 cells (53). At 72 h in single-nucleus cells, TAZ expression decreased but MyoD was still expressed, while in multinuclear cells, both TAZ and MyoD were expressed and colocalized (yellow) in the nuclei (Fig. 4C, DMSO, bottom). IBS008738 did not have a significant effect under growth conditions. However, at 24 h under differentiation conditions, IBS008738 promoted the colocalization of TAZ and MyoD in single-nucleus cells and generated cells with two or three nuclei (Fig. 4C, IBS008738, middle, arrowheads). At 72 h, IBS008738 signifi-

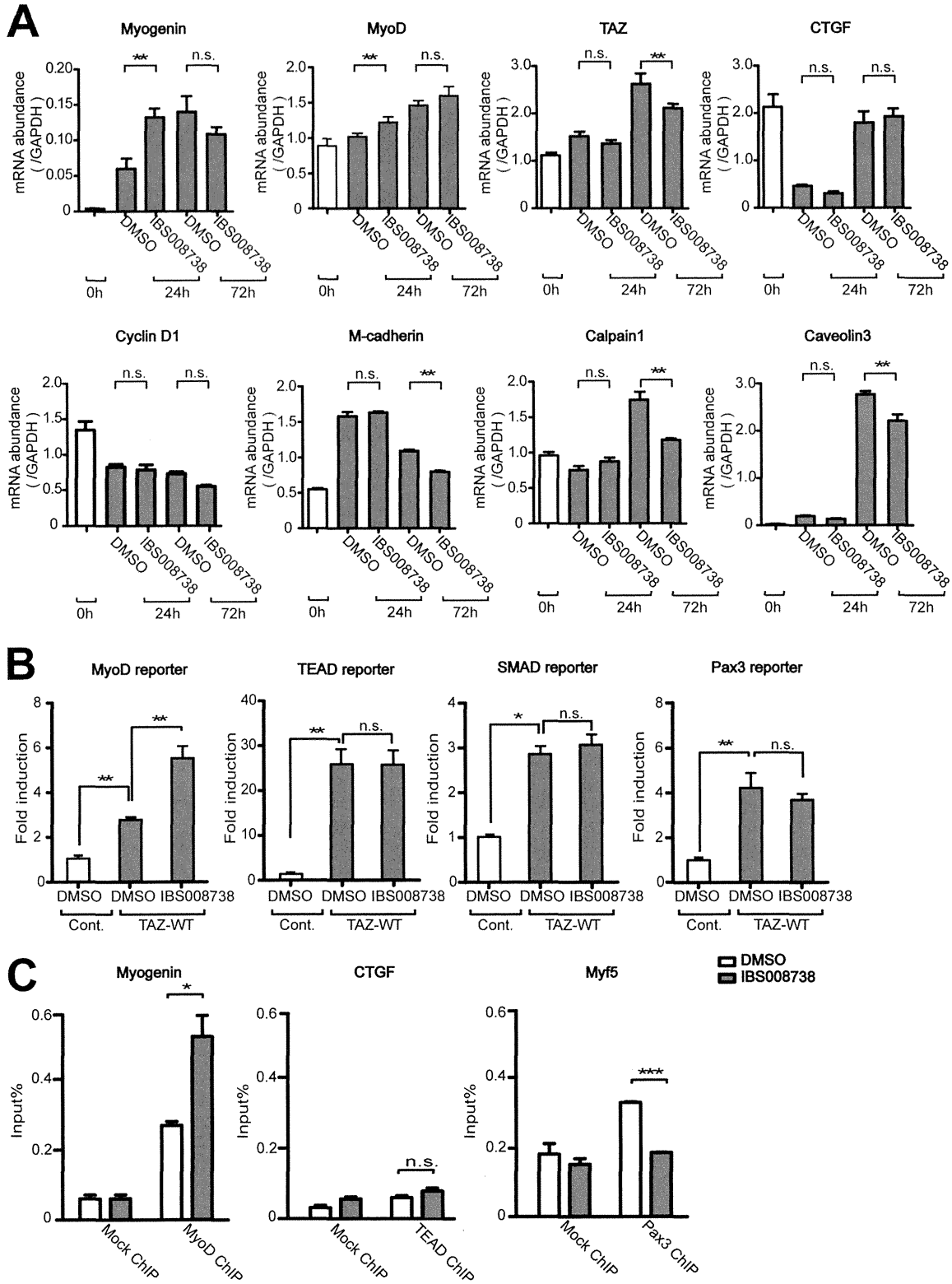

FIG 3 (A) IBS008738 enhances mRNAs of myogenic markers but not of myofusion markers. Quantitative RT-PCR was performed with mRNAs from C2C12 cells just before myogenesis induction (0 h) and from C2C12 cells treated with DMSO or IBS008738 for 24 or 72 h after myogenesis induction (24 h and 72 h). PCR was performed for myogenic markers (myogenin and MyoD), TAZ, putative targets of TAZ (CTGF and cyclin D1), and myofusion markers (M-cadherin, calpain 1, and caveolin 3). (B) IBS008738 enhances the MyoD-responsive myogenin promoter reporter in C2C12 cells. C2C12 cells were transfected with the pGL3 Myo-184-(MyoD), 8×GT-IIC-δ51LucII (for TEAD), 9×CAGA-MLP (for SMAD), and p(PRS-1/-4)3 (for Pax3) luciferase reporters alone (Cont) or with TAZ (TAZ-WT). The cells were grown to confluence and cultured for 24 h under differentiation conditions with DMSO or 10 μM IBS008738. (C) IBS008738 increases the association of MyoD with the myogenin promoter. C2C12 cells were cultured for 24 h under differentiation conditions. ChIP assay was performed with anti-MyoD (MyoD ChIP), anti-TEAD4 (TEAD ChIP), and anti-Pax3 (Pax3 ChIP) antibodies. PCR was performed to detect the promoters of myogenin, CTGF, and Myf5, respectively. Protein G-Sepharose was used as the control (Mock ChIP). In panels A to C, the data are means and standard errors of the means. *, $P < 0.05$; **, $P < 0.01$; ***, $P < 0.001$; n.s., not significant.

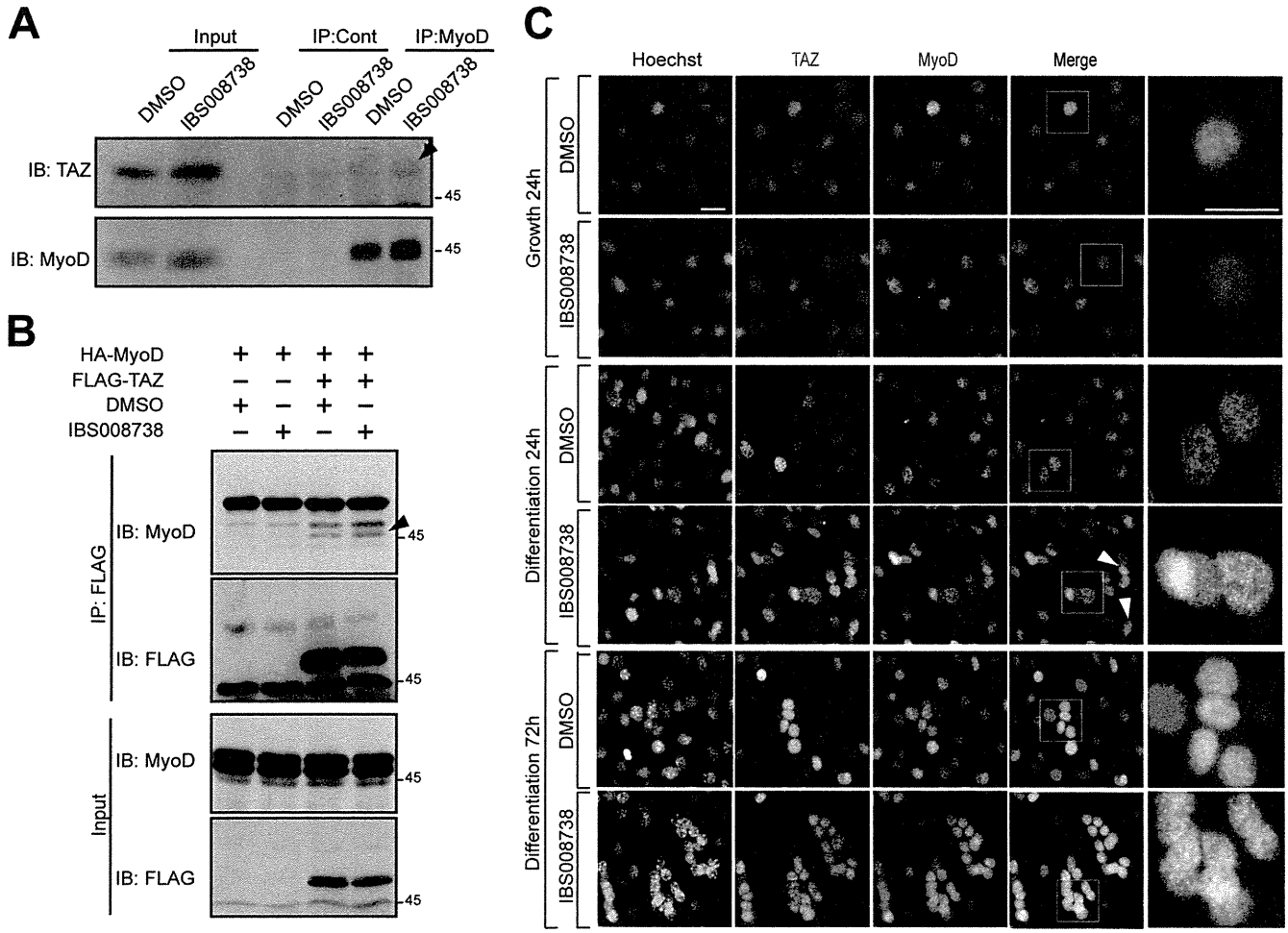

FIG 4 IBS008738 enhances the interaction between TAZ and MyoD. (A) MyoD was immunoprecipitated (IP) from DMSO- or IBS008738-treated C2C12 cells. The inputs and the precipitates were immunoblotted (IB) with anti-TAZ and anti-MyoD antibodies. TAZ immunoprecipitated from the IBS008738-treated cells increased (arrowhead). (B) HA-MyoD and FLAG-TAZ were expressed in HEK293 cells. Immunoprecipitation was performed with anti-FLAG M2 affinity gel. HA-MyoD was coimmunoprecipitated with FLAG-TAZ (third lane). IBS008738 increased the MyoD level in immunoprecipitates (arrowhead). (C) Endogenous MyoD and TAZ were immunostained in C2C12 cells at various stages. MyoD and TAZ were detected in the nuclei at all stages. Under growth conditions, both MyoD and TAZ were distributed diffusely in the nuclei. Under differentiation conditions, MyoD and TAZ formed dots in the nuclei. At 24 h after myogenesis induction, not all of the control cell nuclei expressed MyoD (green) and TAZ (red) equally. During treatment with IBS008738, the merged images are more yellowish, showing that MyoD and TAZ are better colocalized. Arrowheads indicate cells with two or three nuclei. Bar, 50 μm.

cantly increased the percentage of multinuclear cells (Fig. 4C, IBS008738, bottom).

IBS008738 increases the level of unphosphorylated TAZ in C2C12 cells. In epithelial cells, subcellular localization is important in TAZ activity regulation. However, consistent with the immunofluorescence results, in C2C12 cells, TAZ was detected mainly in the nuclear fraction and IBS008738 showed no significant effect on subcellular localization (Fig. 5A). To further characterize the effect of IBS008738 on TAZ, we analyzed TAZ by phosphate affinity SDS-PAGE. TAZ with serine 89 unphosphorylated, which was detected by anti-TAZ antibody (Fig. 5B, left) but not with antibody specific for TAZ with serine 89 phosphorylated (Fig. 5B, right), slightly increased (Fig. 5B, an arrow). However, phosphorylated TAZ also slightly increased, which means that IBS008738 increases the total amount of TAZ. Moreover, phosphorylated and unphosphorylated TAZ from IBS008738-treated cells exhibited mobility different from that of TAZ from control C2C12 cells (Fig. 5B, arrowhead). This finding suggests that in C2C12 cells, even TAZ with serine 89 unphosphorylated is localized in the nucleus and that IBS008738 induces some modification of TAZ, which is distinct from the phosphorylation at serine 89. We also tested the stability of TAZ. In control C2C12 cells, TAZ gradually decreased when protein synthesis was blocked by cycloheximide (Fig. 5C, DMSO). In IBS008738-treated C2C12 cells, TAZ expression was increased and degradation was delayed (Fig. 5C, IBS008738). IBS008738 is likely to stabilize TAZ.

Effect of IBS008738 on TAZ in MCF10A cells. As we used MCF10A cells in the original screening, we wanted to know whether IBS008738 has a similar effect on TAZ in MCF10A cells. The knockdown of TAZ in MCF10A-TAZ cells blocked sphere formation during treatment with IBS008738 (data now shown). Therefore, IBS008738-induced sphere formation indeed depends on TAZ. In the subcellular fractionation of MCF10A-TAZ cells that were cultured under sphere-forming conditions, IBS008738 increased the amount of nuclear TAZ (Fig. 5D, arrowhead). In MCF10A-TAZ cells, IBS008738 enhanced CTGF-encoding gene

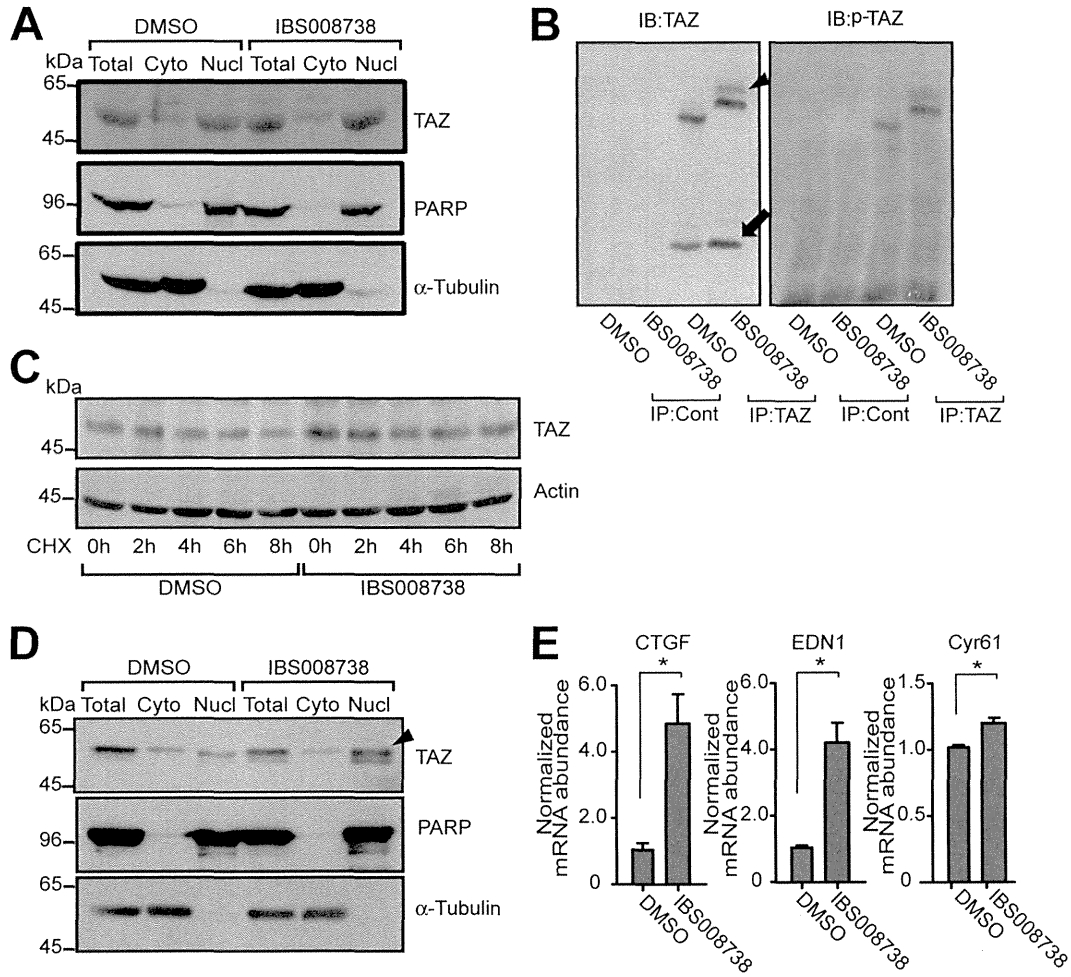

FIG 5 (A) Subcellular TAZ localization in C2C12 cells. Subcellular fractionation of C2C12 cells cultured for 24 h under differentiation conditions was performed. TAZ was recovered mainly in the nuclear fraction. IBS008738 did not significantly influence the distribution of TAZ. PARP and α-tubulin were used as nuclear and cytosolic markers, respectively. (B) TAZ was immunoprecipitated (IP) from lysates of DMSO- and IBS008738-treated C2C12 cells, analyzed by phosphate affinity SDS-PAGE, and immunoblotted with anti-TAZ antibody and anti-serine 89-phosphorylated TAZ-specific antibody, which recognizes the phosphorylation at serine 89. The lower band, which was detected by the anti-TAZ antibody but not by the anti-serine 89-phosphorylated TAZ-specific antibody, increased during treatment with IBS008738 (arrow). The upper bands, which were recognized by anti-serine 89-phosphorylated TAZ-specific antibody, exhibited a different mobility shift with IBS008738 treatment (arrowhead). (C) C2C12 cells were treated with DMSO or 10 μM IBS008738 for 24 h under differentiation conditions and then treated with 50 μg/ml cycloheximide (CHX). TAZ was immunoblotted at the time points indicated. TAZ expression gradually decreased in DMSO-treated C2C12 cells. TAZ expression increased in IBS008738-treated cells, and the decrease was delayed. (D) TAZ in the subcellular fractions of MCF10A-TAZ cells. TAZ was distributed equally in the cytoplasm and the nucleus. IBS008738 increased the nuclear TAZ level (arrowhead). (E) IBS008738 increased the levels of the mRNAs of the TAZ target genes for CTGF, EDN1, and Cyr61 in MCF10A cells. Data are means and standard errors of the means. *, $P < 0.05$.

transcription (Fig. 5E). It also enhanced EDN1 mRNA and to a lesser extent Cyr61 mRNA (Fig. 5E). These findings suggest that IBS008738 increases the nuclear TAZ level in both C2C12 and MCF10A cells but that the genes upregulated are determined in a cell context-dependent manner.

IBS008738 is most effective when applied for the first 24 h under differentiation conditions. To determine the stage at which IBS008738 influences myogenesis, we treated C2C12 cells with the compound at various time points. First, we treated C2C12 cells with various doses of IBS008738 under growth conditions, but IBS008738 had no effect on cell proliferation (Fig. 6A). Next we treated C2C12 cells for various times under differentiation conditions. Treatment during the first 24 h upregulated MHC (Fig. 6B). The expression of myogenin and MyoD was also enhanced (Fig. 6C, arrowheads). In contrast, treatment at 24 to 48 h or 48 to 72 h did not have a significant effect. These findings suggest that IBS008738 is most effective when it is applied during the initial phase of differentiation.

IBS008738 competes with myostatin. Myostatin is a member of the bone morphogenetic protein/transforming growth factor β superfamily and inhibits muscle growth and differentiation. It binds the activin type IIB receptor and triggers SMAD2- and -3-dependent signaling. As TAZ interacts with SMAD2 and -3, we wanted to know whether and how IBS008738 modulates myostatin signaling. Myostatin inhibited myogenesis in C2C12 cells, but IBS008738 restored myogenesis (Fig. 7A, si Cont). TAZ knockdown itself inhibited myogenesis and canceled the effect of IBS008738 (Fig. 7A, si TAZ). The myofusion index corroborated

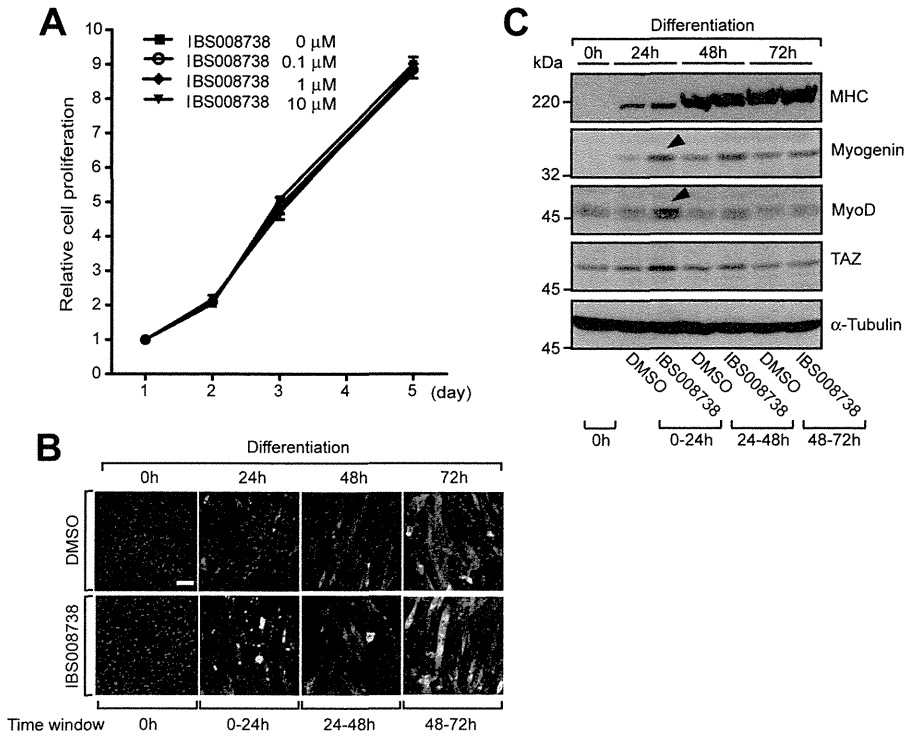

FIG 6 (A) C2C12 cells were cultured under growth conditions with various doses of IBS008738. Viable-cell numbers were evaluated by MTT assay. The value on day 1 after plating was set at 1. IBS008738 had no effect on cell proliferation. (B and C) C2C12 cells under differentiation conditions were treated with 10 μM IBS008738 during the time periods indicated (0 to 24, 24 to 48, and 48 to 72 h). Cells were harvested after treatment (at 24, 48, or 72 h). (B) Immunofluorescence images of MHC (white). Bar, 100 μm. (C) Immunoblotting of MHC, MyoD, myogenin, and TAZ. IBS008738 most significantly enhanced myogenin and MyoD when cells were treated during the first 24 h under differentiation conditions (arrowheads).

the immunofluorescence assay observation (Fig. 7B). In the immunoblotting assay, the MHC level decreased in myostatin-treated cells but IBS008738 restored it (Fig. 7C, second and third lanes). TAZ knockdown attenuated the restoration of MHC expression by IBS008738 (Fig. 7C, fifth and sixth lanes).

IBS008738 facilitates muscle repair in cardiotoxin-injected muscles. To assess the effect of IBS008738 on muscle regeneration, we injected cardiotoxin with control DMSO or IBS008738 into TA muscles. Hematoxylin-eosin staining showed that centrally nucleated fibers, a hallmark of regeneration, increased in IBS008738-injected muscles (Fig. 8A). To quantitatively evaluate muscle fiber size, we immunostained laminin, measured the sizes of myofibers demarcated by laminin, and confirmed the effect of IBS008738 (Fig. 8B). Pax7-positive cells, which were detected under the basal lamina, increased on day 5, decreased on day 7, and returned to the control level on day 14, whereas the number of MyoD-positive cells remained high on days 5 and 7 (Fig. 8C and D). All of these findings support the idea that IBS008738 facilitates muscle regeneration in response to injury.

IBS008738 prevents dexamethasone-induced muscle atrophy. We also induced muscle atrophy by dexamethasone administration in BALB/cByJ mice ($n = 6$ DMSO control, $n = 6$ dexamethasone treated) and injected IBS008738 three times into one hind limb muscle and control DMSO into the contralateral muscle. The mice were sacrificed on day 14. Dexamethasone treatment reduced muscle weights (Fig. 9A, first and third columns). IBS008738 did not increase muscle weights in control mice but prevented a dexamethasone-induced muscle decrease (Fig. 9A, second and fourth columns). Hematoxylin-eosin staining also showed a dexamethasone-induced reduction of muscle fiber size (Fig. 9B, upper panels). IBS008738 itself caused no significant change but prevented dexamethasone-induced muscle atrophy (Fig. 9B, lower panels). A quantitative evaluation of muscle fiber size confirmed the effect of IBS008738 (Fig. 9C). To measure protein synthesis, we injected puromycin 30 min before dexamethasone-treated mice were sacrificed and immunoblotted muscle lysates from the mice ($n = 3$ DMSO control, $n = 3$ IBS008738 treated) with antipuromycin antibody. IBS008738 significantly increased the incorporation of puromycin, suggesting that protein synthesis was enhanced in IBS008738-treated mice (Fig. 9D). Muscle-specific E3 ubiquitin ligases, MuRF-1, and atrogin-1 (MAFbx) are involved in glucocorticoid-induced muscle atrophy (54). Dexamethasone increased the MuRF-1 and atrogin-1 mRNA levels in GM muscles, but IBS008738 decreased them (Fig. 9E). These findings suggest that IBS008738 prevents dexamethasone-induced muscle atrophy through the inhibition of protein degradation and enhancement of protein synthesis.

IBS008738 does not significantly influence the malignant properties of cancer cells. We expect that IBS008738 is a promising lead compound for the development of a drug to prevent muscle atrophy and facilitate muscle regeneration after injury. However, TAZ is known as an oncogene and the hyperactivity of TAZ induces EMT of cancer cells. The effects of IBS008738 on the TEAD and SMAD reporters are not so significant in C2C12 cells, yet we need to consider the risk of IBS008738 application. We tested whether and how IBS008738 induces EMT in cancer cells. It

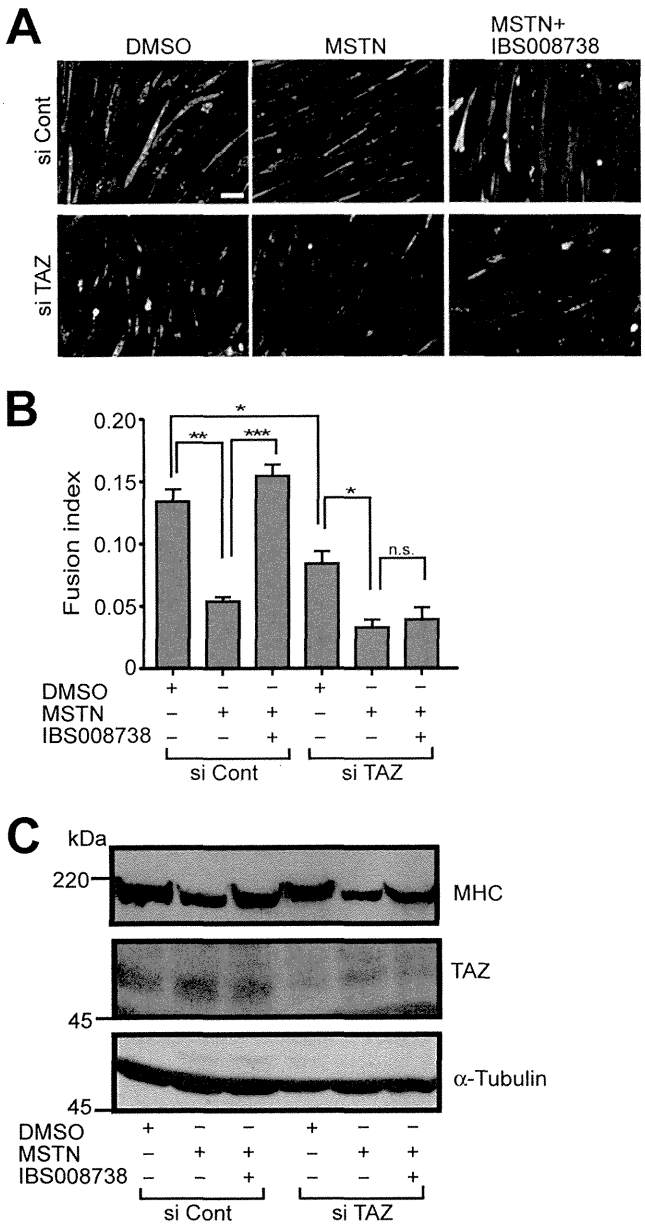

FIG 7 IBS008738 competes with myostatin. C2C12 cells were transfected with control dsRNA (si Cont) or TAZ dsRNA (si TAZ). Cells were grown to confluence and switched to differentiation conditions. Cells were cultured for 72 h with DMSO, 100 ng/ml myostatin (MSTN) alone, or 100 ng/ml myostatin with 10 μM IBS008738 as indicated. (A) Immunofluorescence images of MHC. Bar, 100 μm. (B) Myofusion index. Data are means and standard errors of the means. *, $P < 0.05$; **, $P < 0.01$; ***, $P < 0.001$; n.s., not significant. (C) Cell lysates were immunoblotted with the antibodies indicated.

did not enhance EMT marker protein expression in A431, A549, or HCT116 cells (Fig. 10A). IBS008738 did not enhance tumor sphere formation or the 3D Matrigel growth of A431 cells either (Fig. 10B).

DISCUSSION

In this study, we established a cell-based assay to search for TAZ activators. MCF10A-TAZ SA cells, which are unresponsive to negative regulation by the Hippo pathway, robustly form spheres under mammosphere-forming conditions, while parent MCF10A and MCF10A-TAZ cells lack the capacity to form spheres (Fig. 1). However, LATS1 and LATS2 knockdown makes MCF10A-TAZ cells, but not parent MCF10A cells, form spheres. The additional knockdown of TAZ in MCF10A-TAZ cells with LATS1 and LATS2 knockdown abolished sphere formation. These results indicate that MCF10A-TAZ cells acquire the capacity to form spheres when TAZ is activated. Therefore, we used this assay to identify compounds that activate TAZ. It is not clear which transcriptional factor is implicated in TAZ-dependent sphere formation by MCF10A cells. Among the TAZ-interacting transcriptional factors, TEAD proteins have been shown to be implicated in TAZ-mediated EMT (29). As EMT is related to stemness in cancer cells, genes transcribed by TEAD may be required for sphere formation. Most of the compounds obtained through this assay augment TAZ-dependent upregulation of TEAD-responsive reporter activity in HEK293 cells. The enhancement by the compounds is only 2-fold, but as cells are exposed to the compounds for a longer time in the sphere formation assay, the modest enhancement might be sufficient to induce sphere formation.

This assay gives compounds with disparate targets. The regulation of TAZ is multifaceted. The Hippo pathway, junction proteins, the actin cytoskeleton, and the Wnt pathway regulate TAZ. The compounds may upregulate TAZ through these regulatory mechanisms. Our preliminary experiments suggest that the compounds show different effects on the differentiation of mouse mesenchymal stem cells (data not shown). Some compounds strongly promote osteogenesis, while others do not. The inhibitory effects on adipogenesis are also unequal. These findings support the idea that each compound activates TAZ through a distinct mechanism. YAP1 is a paralog of TAZ. The molecular structures of YAP1 and TAZ are similar. YAP1 is regulated by the Hippo pathway, junction proteins, and the actin cytoskeleton in a manner similar to that of TAZ regulation (3, 12, 13). If the compounds work through the same regulatory mechanisms, the compounds should activate YAP1 too. Indeed, some of them enhance YAP1-dependent TEAD-responsive reporter activity, but not all of the compounds are active for YAP1. This observation also implies that the targets of 50 TAZ activator candidates are not the same. Thus, this new cell-based assay provided us with a collection of 50 TAZ activator candidate compounds that exhibit various cellular outputs and have distinct molecular targets.

As TAZ promotes osteogenesis and inhibits adipogenesis in mesenchymal stem cells, it is tempting to use TAZ activators therapeutically against osteoporosis and obesity. The osteogenic and antiadipogenic effects of kaempferol, a dietary flavonoid, depend on TAZ, supporting the notion that TAZ can be a therapeutic target in osteoporosis and obesity (55). Accordingly, the TAZ activator TM-25659 has been proposed to be beneficial in the control of osteoporosis and obesity (56). However, in the treatment of osteoporosis, the patients are females after menopause and relatively young. Once drug application starts, it is not easy to stop it. The oncogenic property of TAZ is an obstacle in the application of TAZ activators to osteoporosis. In the treatment of sarcopenia, the patients are extremely old. Once sufficient muscles are acquired for the rehabilitation program, the drug can be withdrawn. As the recovery of lower limb muscles is the most important, local application to those muscles by injection or percutaneously might be sufficient and systemic application could be avoided. Therefore, we expect that the treatment of sarcopenia with TAZ activators is

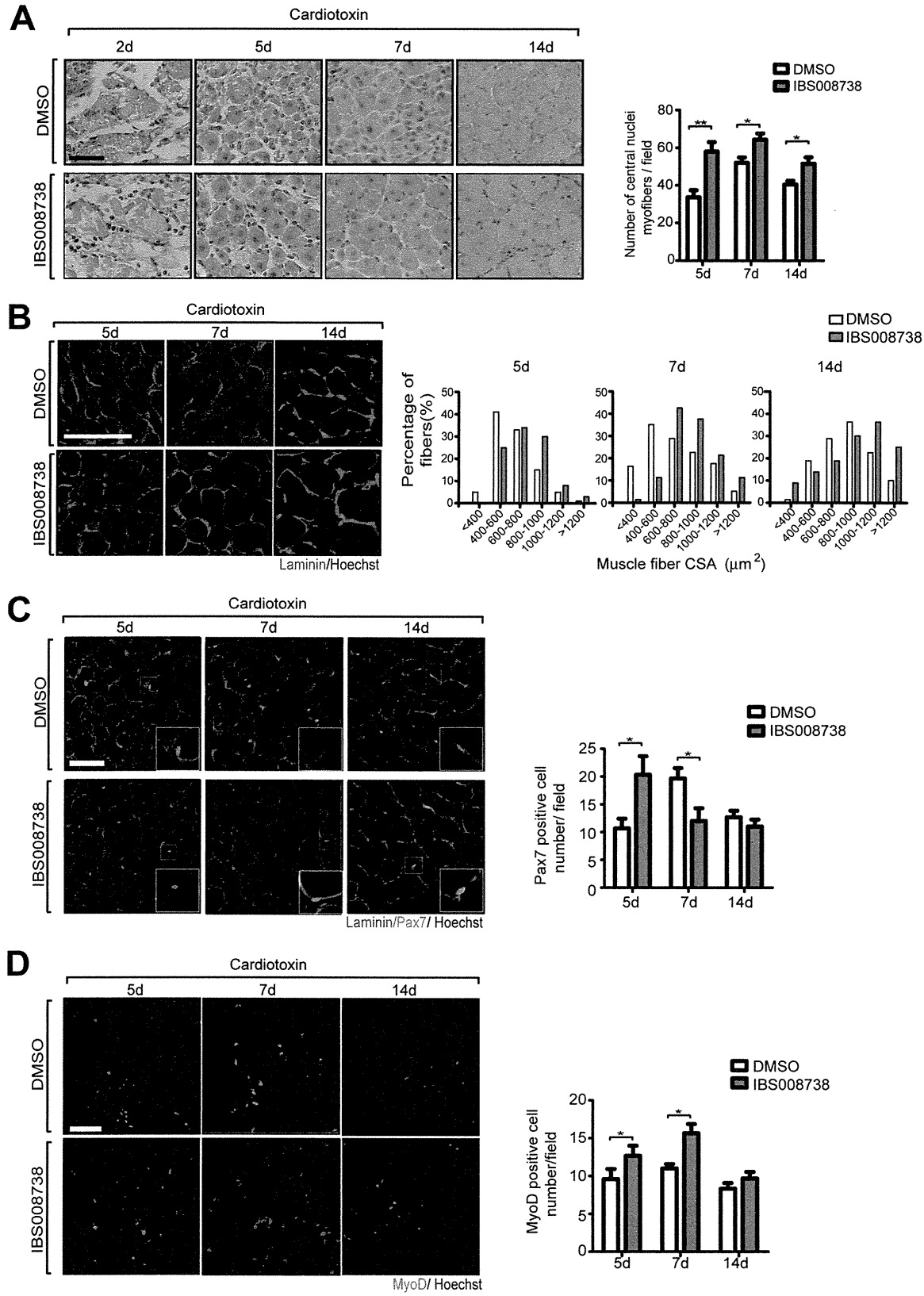

FIG 8 IBS008738 facilitates the repair of cardiotoxin-injected muscles. (A) Cardiotoxin was injected into TA muscles with control DMSO or IBS008738. The muscles were fixed at the time points indicated. The centrally nucleated fibers in nine independent fields of each muscle were counted at ×20 magnification. (B) Tissues were immunostained with antilaminin antibody. Cross-sectional areas (CSA) of myofibers were measured. Five hundred myofibers in each mouse sample were analyzed. Data from three mice are shown. (C and D) Tissues were immunostained with anti-Pax7 (red) and antilaminin (green) antibodies in panel C and with anti-MyoD antibody (red) in panel D at the time points indicated. In panel C, the marked fields are shown at higher magnification in the insets. The Pax7- and MyoD-positive cells in six independent fields of each muscle were counted at ×20 magnification. The data summarize the results obtained from three mice. In panels A, C, and D, the data are means and standard errors of the means. *, $P < 0.05$; **, $P < 0.01$. Bar, 50 μm.

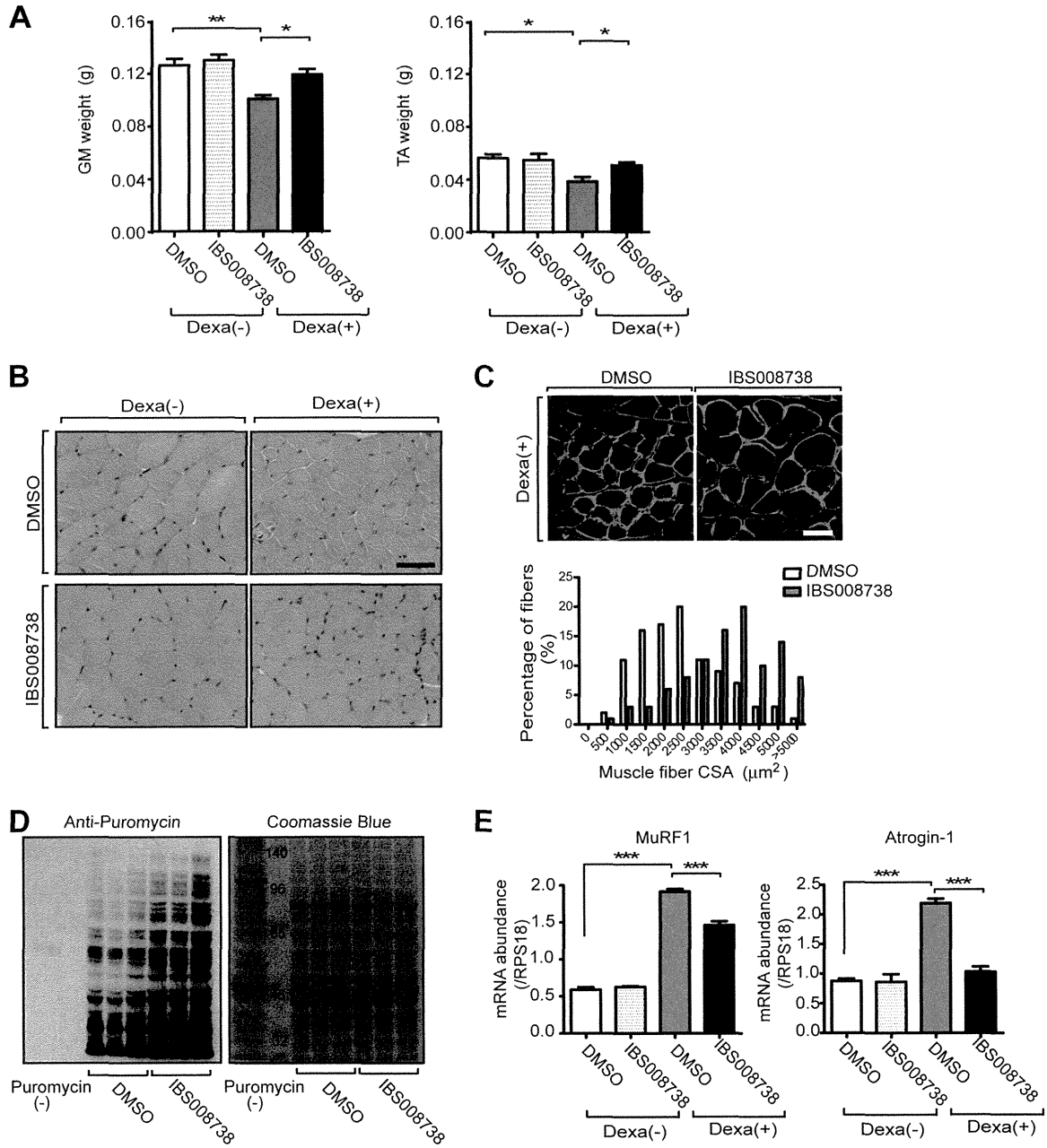

FIG 9 IBS008738 prevents dexamethasone-induced muscle atrophy. Dexamethasone (Dexa; 25 mg/kg/day) was intraperitoneally injected into 6-week-old female BALB/cByJ mice for 1 week. Control DMSO or IBS008738 was injected into their hind limbs every other day. On day 14, muscles were fixed. (A) Weights of GM and TA muscles. (B) Tissues were stained with hematoxylin and eosin. Dexamethasone induced muscle atrophy (upper panels). IBS008738 partially blocked atrophy (lower panels). Bar, 50 μm. (C) Cross-sectional areas (CSA) of myofibers were analyzed as described in the legend to Fig. 8B. (D) Puromycin was injected intraperitoneally 30 min before dexamethasone-treated mice were sacrificed. Puromycin-labeled proteins in GM muscles were detected with antipuromycin antibody (left panel). Samples of three DMSO-treated and three IBS008738-treated muscles were run side by side. A sample from a mouse with no injection of puromycin was run in the first lane. To confirm that the same amount of proteins was run in each lane, the membranes were stained with Coomassie brilliant blue (right panel). (E) Quantitative RT-PCR was performed with mRNAs from GM muscles. IBS008738 partially suppressed the dexamethasone-induced increase in the MuRF-1 and atrogin-1 mRNAs. In panels A and E, the data are means and standard errors of the means. *, $P < 0.05$; **, $P < 0.01$; ***, $P < 0.001$.

more realistic. Hence, we selected compounds that facilitate myogenesis in mouse C2C12 myoblast cells and expected that such compounds may also promote satellite cell proliferation and differentiation. In this study, we focused on one compound, IBS008738.

The effects of IBS008738 on sphere formation by MCF10A-TAZ cells and myogenesis of C2C12 cells are both abolished by TAZ knockdown. This indicates that the effect of IBS008738 depends on TAZ. In MCF10A-TAZ cells, IBS008738 increases the nuclear TAZ level (Fig. 5). In C2C12 cells, IBS008738 increases the

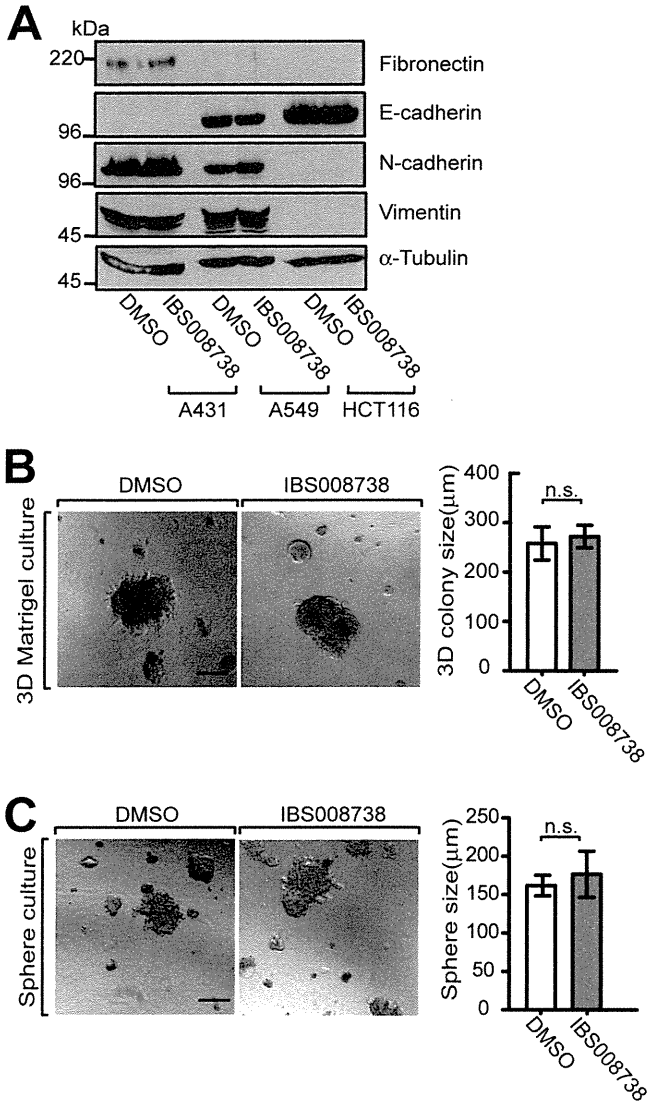

FIG 10 Effect of IBS008738 on cancer cells. (A) Human epidermal cancer A431, lung cancer A549, and colon cancer HCT116 cells were treated with IBS008738. Cell lysates were immunoblotted with the antibodies indicated. (B and C) A431 cells were cultured under sphere-forming conditions (B) or in 3D Matrigel (C). The maximum diameters of 30 cell aggregates with diameters of >150 μm were measured. IBS008738 did not enhance tumor sphere formation or the growth of A431 cells in 3D Matrigel. Bar, 200 μm. In panels B and C, the data are means and standard errors of the means. n.s., not significant.

unphosphorylated TAZ level. These changes also support the idea that IBS008738 indeed works on TAZ. Phosphate affinity SDS-PAGE analysis suggests that IBS008738 induces modifications of TAZ other than phosphorylation at serine 89. It will be intriguing and necessary to determine the molecular modifications by mass spectrometry. Phosphate affinity SDS-PAGE has additionally revealed that almost 50% of the TAZ in C2C12 cells is phosphorylated but that most of the TAZ is localized in the nucleus. This finding implies that the phosphorylated TAZ in C2C12 cells cannot be captured in the cytoplasm or is retained by the nucleus. This might be due to the limited amount of 14-3-3 or the abundance of nuclear transcriptional factors such as MyoD that interact with TAZ. The effects of IBS008738 on gene transcription are different in MCF10A and C2C12 cells. IBS008738 increases CTGF mRNA in MCF10A cells but not in C2C12 cells (Fig. 3). Likewise, IBS008738 enhances TEAD-responsive reporter activity in HEK293 cells but not in C2C12 cells. These discrepancies may reflect the different expression of TEAD and MyoD in these cells, and TAZ may select the interacting partners in a cell context-dependent manner. On the basis of our reporter and ChIP assays, we speculate that in C2C12 cells, MyoD is the main partner of TAZ under differentiation conditions and that consequently MyoD-mediated cellular outputs are most prominent in IBS008738-treated C2C12 cells.

IBS008738 enhances MyoD expression in C2C12 cells under growth conditions and accelerates myogenesis under differentiation conditions (Fig. 2). The *in vitro* interaction experiment and the immunofluorescence assay support the idea that IBS008738 augments the association of TAZ with MyoD (Fig. 4). IBS008738 stabilizes TAZ and increases its protein expression (Fig. 5). IBS008738 promotes the association of MyoD with the myogenin promoter (Fig. 3C). The binding of Pax3 to the Myf5 promoter decreased in IBS008738-treated cells. This finding is understandable, because Myf5 is known to be downregulated early in differentiation (53). As the ChIP assay was performed 24 h after differentiation, we speculated that this decrease may mirror the rapid myogenesis that occurs during IBS008738 treatment. The competition of IBS008738 with myostatin is equivocal. As SMAD2 and -3 mediate myostatin signaling and TAZ cooperates with SMAD2 and -3 in human embryonic stem cells and mouse embryos, TAZ activators are postulated to enhance myostatin signaling but IBS008738 competes with myostatin in the myogenesis of C2C12 cells (Fig. 7). We here infer again that the effect of IBS008738 on MyoD is more prominent because MyoD is more abundant than SMAD2 and -3 in C2C12 cells.

IBS008738 increases the numbers of Pax7-positive cells in the early phase and centrally nucleated fibers in injured muscles. Later, the number of Pax7-positive cells decreases while that of MyoD-positive cells increases (Fig. 8). Pax7 is thought to play dual roles in the regeneration of skeletal muscles (57). Pax7 promotes progenitors to commit to the skeletal muscle lineage but blocks terminal differentiation. Heterogeneity of satellite cells has also been discussed (58). Ten percent of quiescent satellite stem cells are $Pax7^+$ $Myf5^-$, whereas 90% of committed quiescent satellite cells are $Pax7^+$ $Myf5^+$ and are activated to subsequently coexpress MyoD, undergo limited proliferation, and then differentiate into $Pax7^-$ $MyoD^+$ cells (58, 59). We could not identify which Pax7-positive cells IBS008738 increased in the early phase after injury. We speculate the IBS008738 promotes both self-renewal of satellite stem cells and the commitment to $Pax7^+$ $Myf5^+$ satellite cells in response to injury and that it also promotes myogenic differentiation to $Pax7^+$ $Myf5^+$ $MyoD^+$ cells, which further differentiate to $Pax7^-$ $MyoD^+$ cells and at the same time harbor the subpopulation that returns to quiescent satellite cells. Thus, IBS008738 overall facilitates muscle repair with the replenishment of satellite cells. However, in order to understand how IBS008738 works, a more detailed analysis of the role of TAZ in satellite cells is necessary. IBS008738 also prevents dexamethasone-induced muscle atrophy. IBS008738 suppresses the expression of MuRF-1 and atrogin-1 and increases protein synthesis (Fig. 9). On the other hand, IBS008738 does not significantly induce EMT in the cancer cells tested (Fig. 10). These observations imply that IBS008738 may be useful for the treatment and prevention of muscle atrophy.

In this paper, we have introduced a novel cell-based assay to screen for TAZ activators. As compounds with various targets and a wide spectrum of cellular phenotypes are obtained with this assay, the collection works as a minilibrary of TAZ activators. Researchers can perform further selection based on the different cellular outputs as readouts and obtain compounds that function according to their interests.

ACKNOWLEDGMENTS

We are grateful for Hiroshi Asahara (Tokyo Medical and Dental University), Yasutomi Kamei (Kyoto Prefectural University), Hiroki Kurihara (The University of Tokyo), Yoshihiro Ogawa (Tokyo Medical and Dental University), Hiroshi Sasaki (Kumamoto University), Kenji Miyazawa (Yamanashi University), Kohei Miyazono (The University of Tokyo), Hiroshi Takayanagi (The University of Tokyo), and Sumiko Watanabe (The University of Tokyo) for materials and advice.

This work was supported by research grants from the Ministry of Education, Sports, Science, and Technology (17081008), the Japan Society for the Promotion of Science (22790275 and 22590267), the Suzuken Memorial Foundation, the Nakatomi Foundation, the Uehara Memorial Foundation, and the Naito Foundation. Z.Y. was supported by a Japanese Government (Monbukagakusho) (MEXT) scholarship.

REFERENCES

1. **Kanai F, Marignani PA, Sarbassova D, Yagi R, Hall RA, Donowitz M, Hisaminato A, Fujiwara T, Ito Y, Cantley LC, Yaffe MB.** 2000. TAZ: a novel transcriptional co-activator regulated by interactions with 14-3-3 and PDZ domain proteins. EMBO J. **19**:6778–6791. http://dx.doi.org/10.1093/emboj/19.24.6778.
2. **Hong W, Guan KL.** 2012. The YAP and TAZ transcription co-activators: key downstream effectors of the mammalian Hippo pathway. Semin. Cell Dev. Biol. **23**:785–793. http://dx.doi.org/10.1016/j.semcdb.2012.05.004.
3. **Wang K, Degerny C, Xu M, Yang XJ.** 2009. YAP, TAZ, and Yorkie: a conserved family of signal-responsive transcriptional coregulators in animal development and human disease. Biochem. Cell Biol. **87**:77–91. http://dx.doi.org/10.1139/O08-114.
4. **Sudol M.** 1994. Yes-associated protein (YAP65) is a proline-rich phosphoprotein that binds to the SH3 domain of the Yes proto-oncogene product. Oncogene **9**:2145–2152.
5. **Bao Y, Hata Y, Ikeda M, Withanage K.** 2011. Mammalian Hippo pathway: from development to cancer and beyond. J. Biochem. **149**:361–379. http://dx.doi.org/10.1093/jb/mvr021.
6. **Pan D.** 2010. The Hippo signaling pathway in development and cancer. Dev. Cell **19**:491–505. http://dx.doi.org/10.1016/j.devcel.2010.09.011.
7. **Oka T, Remue E, Meerschaert K, Vanloo B, Boucherie C, Gfeller D, Bader GD, Sidhu SS, Vandekerckhove J, Gettemans J, Sudol M.** 2010. Functional complexes between YAP2 and ZO-2 are PDZ domain-dependent, and regulate YAP2 nuclear localization and signalling. Biochem. J. **432**:461–472. http://dx.doi.org/10.1042/BJ20100870.
8. **Remue E, Meerschaert K, Oka T, Boucherie C, Vandekerckhove J, Sudol M, Gettemans J.** 2010. TAZ interacts with zonula occludens-1 and -2 proteins in a PDZ-1 dependent manner. FEBS Lett. **584**:4175–4180. http://dx.doi.org/10.1016/j.febslet.2010.09.020.
9. **Chan SW, Lim CJ, Chong YF, Pobbati AV, Huang C, Hong W.** 2011. Hippo pathway-independent restriction of TAZ and YAP by angiomotin. J. Biol. Chem. **286**:7018–7026. http://dx.doi.org/10.1074/jbc.C110.212621.
10. **Zhao B, Li L, Lu Q, Wang LH, Liu CY, Lei Q, Guan KL.** 2011. Angiomotin is a novel Hippo pathway component that inhibits YAP oncoprotein. Genes Dev. **25**:51–63. http://dx.doi.org/10.1101/gad.2000111.
11. **Dupont S, Morsut L, Aragona M, Enzo E, Giulitti S, Cordenonsi M, Zanconato F, Le Digabel J, Forcato M, Bicciato S, Elvassore N, Piccolo S.** 2011. Role of YAP/TAZ in mechanotransduction. Nature **474**:179–183. http://dx.doi.org/10.1038/nature10137.
12. **Halder G, Dupont S, Piccolo S.** 2012. Transduction of mechanical and cytoskeletal cues by YAP and TAZ. Nat. Rev. Mol. Cell Biol. **13**:591–600. http://dx.doi.org/10.1038/nrm3416.
13. **Wrighton KH.** 2011. Mechanotransduction: YAP and TAZ feel the force. Nat. Rev. Mol. Cell Biol. **12**:404. http://dx.doi.org/10.1038/nrm3145, http://dx.doi.org/10.1038/nrm3136.
14. **Azzolin L, Zanconato F, Bresolin S, Forcato M, Basso G, Bicciato S, Cordenonsi M, Piccolo S.** 2012. Role of TAZ as mediator of Wnt signaling. Cell **151**:1443–1456. http://dx.doi.org/10.1016/j.cell.2012.11.027.
15. **Imajo M, Miyatake K, Iimura A, Miyamoto A, Nishida E.** 2012. A molecular mechanism that links Hippo signalling to the inhibition of Wnt/β-catenin signalling. EMBO J. **31**:1109–1122. http://dx.doi.org/10.1038/emboj.2011.487.
16. **Varelas X, Miller BW, Sopko R, Song S, Gregorieff A, Fellouse FA, Sakuma R, Pawson T, Hunziker W, McNeill H, Wrana JL, Attisano L.** 2010. The Hippo pathway regulates Wnt/beta-catenin signaling. Dev. Cell **18**:579–591. http://dx.doi.org/10.1016/j.devcel.2010.03.007.
17. **de Cristofaro T, Di Palma T, Ferraro A, Corrado A, Lucci V, Franco R, Fusco A, Zannini M.** 2011. TAZ/WWTR1 is overexpressed in papillary thyroid carcinoma. Eur. J. Cancer **47**:926–933. http://dx.doi.org/10.1016/j.ejca.2010.11.008.
18. **Wang L, Shi S, Guo Z, Zhang X, Han S, Yang A, Wen W, Zhu Q.** 2013. Overexpression of YAP and TAZ is an independent predictor of prognosis in colorectal cancer and related to the proliferation and metastasis of colon cancer cells. PLoS One **8**:e65539. http://dx.doi.org/10.1371/journal.pone.0065539.
19. **Wei Z, Wang Y, Li Z, Yuan C, Zhang W, Wang D, Ye J, Jiang H, Wu Y, Cheng J.** 29 March 2013. Overexpression of Hippo pathway effector TAZ in tongue squamous cell carcinoma: correlation with clinicopathological features and patients' prognosis. J. Oral Pathol. Med. (Epub ahead of print.) http://dx.doi.org/10.1111/jop.12062.
20. **Yuen HF, McCrudden CM, Huang YH, Tham JM, Zhang X, Zeng Q, Zhang SD, Hong W.** 2013. TAZ expression as a prognostic indicator in colorectal cancer. PLoS One **8**:e54211. http://dx.doi.org/10.1371/journal.pone.0054211.
21. **Zhou Z, Hao Y, Liu N, Raptis L, Tsao MS, Yang X.** 2011. TAZ is a novel oncogene in non-small cell lung cancer. Oncogene **30**:2181–2186. http://dx.doi.org/10.1038/onc.2010.606.
22. **Bhat KP, Salazar KL, Balasubramaniyan V, Wani K, Heathcock L, Hollingsworth F, James JD, Gumin J, Diefes KL, Kim SH, Turski A, Azodi Y, Yang Y, Doucette T, Colman H, Sulman EP, Lang FF, Rao G, Copray S, Vaillant BD, Aldape KD.** 2011. The transcriptional coactivator TAZ regulates mesenchymal differentiation in malignant glioma. Genes Dev. **25**:2594–2609. http://dx.doi.org/10.1101/gad.176800.111.
23. **Chan SW, Lim CJ, Guo K, Ng CP, Lee I, Hunziker W, Zeng Q, Hong W.** 2008. A role for TAZ in migration, invasion, and tumorigenesis of breast cancer cells. Cancer Res. **68**:2592–2598. http://dx.doi.org/10.1158/0008-5472.CAN-07-2696.
24. **Cordenonsi M, Zanconato F, Azzolin L, Forcato M, Rosato A, Frasson C, Inui M, Montagner M, Parenti AR, Poletti A, Daidone MG, Dupont S, Basso G, Bicciato S, Piccolo S.** 2011. The Hippo transducer TAZ confers cancer stem cell-related traits on breast cancer cells. Cell **147**:759–772. http://dx.doi.org/10.1016/j.cell.2011.09.048.
25. **Hao J, Zhang Y, Jing D, Li Y, Li J, Zhao Z.** 2014. Role of Hippo signaling in cancer stem cells. J. Cell Physiol. **229**:266–270. http://dx.doi.org/10.1002/jcp.24455.
26. **Skinner M.** 2012. Cancer stem cells: TAZ takes centre stage. Nat. Rev. Cancer **12**:82–83. http://dx.doi.org/10.1038/nrc3210.
27. **Chan SW, Lim CJ, Huang C, Chong YF, Gunaratne HJ, Hogue KA, Blackstock WP, Harvey KF, Hong W.** 2011. WW domain-mediated interaction with Wbp2 is important for the oncogenic property of TAZ. Oncogene **30**:600–610. http://dx.doi.org/10.1038/onc.2010.438.
28. **Chan SW, Lim CJ, Loo LS, Chong YF, Huang C, Hong W.** 2009. TEADs mediate nuclear retention of TAZ to promote oncogenic transformation. J. Biol. Chem. **284**:14347–14358. http://dx.doi.org/10.1074/jbc.M901568200.
29. **Zhang H, Liu CY, Zha ZY, Zhao B, Yao J, Zhao S, Xiong Y, Lei QY, Guan KL.** 2009. TEAD transcription factors mediate the function of TAZ in cell growth and epithelial-mesenchymal transition. J. Biol. Chem. **284**:13355–13362. http://dx.doi.org/10.1074/jbc.M900843200.
30. **Park KS, Whitsett JA, Di Palma T, Hong JH, Yaffe MB, Zannini M.** 2004. TAZ interacts with TTF-1 and regulates expression of surfactant protein-C. J. Biol. Chem. **279**:17384–17390. http://dx.doi.org/10.1074/jbc.M312569200.
31. **Murakami M, Nakagawa M, Olson EN, Nakagawa O.** 2005. A WW domain protein TAZ is a critical coactivator for TBX5, a transcription factor implicated in Holt-Oram syndrome. Proc. Natl. Acad. Sci. U. S. A. **102**:18034–18039. http://dx.doi.org/10.1073/pnas.0509109102.
32. **Varelas X, Sakuma R, Samavarchi-Tehrani P, Peerani R, Rao BM,**

Dembowy J, Yaffe MB, Zandstra PW, Wrana JL. 2008. TAZ controls Smad nucleocytoplasmic shuttling and regulates human embryonic stem-cell self-renewal. Nat. Cell Biol. **10**:837–848. http://dx.doi.org/10.1038/ncb1748.

33. **Varelas X, Samavarchi-Tehrani P, Narimatsu M, Weiss A, Cockburn K, Larsen BG, Rossant J, Wrana JL.** 2010. The Crumbs complex couples cell density sensing to Hippo-dependent control of the TGF-β-SMAD pathway. Dev. Cell **19**:831–844. http://dx.doi.org/10.1016/j.devcel.2010.11.012.
34. **Hong JH, Hwang ES, McManus MT, Amsterdam A, Tian Y, Kalmukova R, Mueller E, Benjamin T, Spiegelman BM, Sharp PA, Hopkins N, Yaffe MB.** 2005. TAZ, a transcriptional modulator of mesenchymal stem cell differentiation. Science **309**:1074–1078. http://dx.doi.org/10.1126/science.1110955.
35. **Cui CB, Cooper LF, Yang X, Karsenty G, Aukhil I.** 2003. Transcriptional coactivation of bone-specific transcription factor Cbfa1 by TAZ. Mol. Cell. Biol. **23**:1004–1013. http://dx.doi.org/10.1128/MCB.23.3.1004-1013.2003.
36. **Jeong H, Bae S, An SY, Byun MR, Hwang JH, Yaffe MB, Hong JH, Hwang ES.** 2010. TAZ as a novel enhancer of MyoD-mediated myogenic differentiation. FASEB J. **24**:3310–3320. http://dx.doi.org/10.1096/fj.09-151324.
37. **Murakami M, Tominaga J, Makita R, Uchijima Y, Kurihara Y, Nakagawa O, Asano T, Kurihara H.** 2006. Transcriptional activity of Pax3 is co-activated by TAZ. Biochem. Biophys. Res. Commun. **339**:533–539. http://dx.doi.org/10.1016/j.bbrc.2005.10.214.
38. **Benhaddou A, Keime C, Ye T, Morlon A, Michel I, Jost B, Mengus G, Davidson I.** 2012. Transcription factor TEAD4 regulates expression of myogenin and the unfolded protein response genes during C2C12 cell differentiation. Cell Death Differ. **19**:220–231. http://dx.doi.org/10.1038/cdd.2011.87.
39. **Zhu X, Topouzis S, Liang LF, Stotish RL.** 2004. Myostatin signaling through Smad2, Smad3 and Smad4 is regulated by the inhibitory Smad7 by a negative feedback mechanism. Cytokine **26**:262–272. http://dx.doi.org/10.1016/j.cyto.2004.03.007.
40. **Judson RN, Gray SR, Walker C, Carroll AM, Itzstein C, Lionikas A, Zammit PS, De Bari C, Wackerhage H.** 2013. Constitutive expression of Yes-associated protein (Yap) in adult skeletal muscle fibres induces muscle atrophy and myopathy. PLoS One **8**:e59622. http://dx.doi.org/10.1371/journal.pone.0059622.
41. **Watt KI, Judson R, Medlow P, Reid K, Kurth TB, Burniston JG, Ratkevicius A, De Bari C, Wackerhage H.** 2010. Yap is a novel regulator of C2C12 myogenesis. Biochem. Biophys. Res. Commun. **393**:619–624. http://dx.doi.org/10.1016/j.bbrc.2010.02.034.
42. **Sayer AA, Robinson SM, Patel HP, Shavlakadze T, Cooper C, Grounds MD.** 2013. New horizons in the pathogenesis, diagnosis and management of sarcopenia. Age Ageing **42**:145–150. http://dx.doi.org/10.1093/ageing/afs191.
43. **Bao Y, Nakagawa K, Yang Z, Ikeda M, Withanage K, Ishigami-Yuasa M, Okuno Y, Hata S, Nishina H, Hata Y.** 2011. A cell-based assay to screen stimulators of the Hippo pathway reveals the inhibitory effect of dobutamine on the YAP-dependent gene transcription. J. Biochem. **150**:199–208. http://dx.doi.org/10.1093/jb/mvr063.
44. **Ikeda M, Kawata A, Nishikawa M, Tateishi Y, Yamaguchi M, Nakagawa K, Hirabayashi S, Bao Y, Hidaka S, Hirata Y, Hata Y.** 2009. Hippo pathway-dependent and -independent roles of RASSF6. Sci. Signal. **2**:ra59. http://dx.doi.org/10.1126/scisignal.2000300.
45. **Hirabayashi S, Nakagawa K, Sumita K, Hidaka S, Kawai T, Ikeda M, Kawata A, Ohno K, Hata Y.** 2008. Threonine 74 of MOB1 is a putative key phosphorylation site by MST2 to form the scaffold to activate nuclear Dbf2-related kinase 1. Oncogene **27**:4281–4292. http://dx.doi.org/10.1038/onc.2008.66.
46. **Bao Y, Sumita K, Kudo T, Withanage K, Nakagawa K, Ikeda M, Ohno K, Wang Y, Hata Y.** 2009. Roles of mammalian sterile 20-like kinase 2-dependent phosphorylations of Mps one binder 1B in the activation of nuclear Dbf2-related kinases. Genes Cells **14**:1369–1381. http://dx.doi.org/10.1111/j.1365-2443.2009.01354.x.
47. **Ota M, Sasaki H.** 2008. Mammalian Tead proteins regulate cell proliferation and contact inhibition as transcriptional mediators of Hippo signaling. Development **135**:4059–4069. http://dx.doi.org/10.1242/dev.027151.
48. **Kobayashi N, Goto K, Horiguchi K, Nagata M, Kawata M, Miyazawa K, Saitoh M, Miyazono K.** 2007. c-Ski activates MyoD in the nucleus of myoblastic cells through suppression of histone deacetylases. Genes Cells **12**:375–385. http://dx.doi.org/10.1111/j.1365-2443.2007.01052.x.
49. **Nelson JD, Denisenko O, Bomsztyk K.** 2006. Protocol for the fast chromatin immunoprecipitation (ChIP) method. Nat. Protoc. **1**:179–185. http://dx.doi.org/10.1038/nprot.2006.27.
50. **Goodman CA, Mabrey DM, Frey JW, Miu MH, Schmidt EK, Pierre P, Hornberger TA.** 2011. Novel insights into the regulation of skeletal muscle protein synthesis as revealed by a new nonradioactive in vivo technique. FASEB J. **25**:1028–1039. http://dx.doi.org/10.1096/fj.10-168799.
51. **Ikeda M, Hirabayashi S, Fujiwara N, Mori H, Kawata A, Iida J, Bao Y, Sato Y, Iida T, Sugimura H, Hata Y.** 2007. Ras-association domain family protein 6 induces apoptosis via both caspase-dependent and caspase-independent pathways. Exp. Cell Res. **313**:1484–1495. http://dx.doi.org/10.1016/j.yexcr.2007.02.013.
52. **Hong JH, Yaffe MB.** 2006. TAZ: a beta-catenin-like molecule that regulates mesenchymal stem cell differentiation. Cell Cycle **5**:176–179. http://dx.doi.org/10.4161/cc.5.2.2362.
53. **Lindon C, Montarras D, Pinset C.** 1998. Cell cycle-regulated expression of the muscle determination factor Myf5 in proliferating myoblasts. J. Cell Biol. **140**:111–118. http://dx.doi.org/10.1083/jcb.140.1.111.
54. **Schakman O, Kalista S, Barbé C, Loumaye A, Thissen JP.** 2013. Glucocorticoid-induced skeletal muscle atrophy. Int. J. Biochem. Cell Biol. **45**:2163–2172. http://dx.doi.org/10.1016/j.biocel.2013.05.036.
55. **Byun MR, Jeong H, Bae SJ, Kim AR, Hwang ES, Hong JH.** 2012. TAZ is required for the osteogenic and anti-adipogenic activities of kaempferol. Bone **50**:364–372. http://dx.doi.org/10.1016/j.bone.2011.10.035.
56. **Jang EJ, Jeong H, Kang JO, Kim NJ, Kim MS, Choi SH, Yoo SE, Hong JH, Bae MA, Hwang ES.** 2012. TM-25659 enhances osteogenic differentiation and suppresses adipogenic differentiation by modulating the transcriptional co-activator TAZ. Br. J. Pharmacol. **165**:1584–1594. http://dx.doi.org/10.1111/j.1476-5381.2011.01664.x.
57. **Olguín HC, Pisconti A.** 2012. Marking the tempo for myogenesis: Pax7 and the regulation of muscle stem cell fate decisions. J. Cell. Mol. Med. **16**:1013–1025. http://dx.doi.org/10.1111/j.1582-4934.2011.01348.x.
58. **Wang YX, Rudnicki MA.** 2012. Satellite cells, the engines of muscle repair. Nat. Rev. Mol. Cell Biol. **13**:127–133. http://dx.doi.org/10.1038/nrm3265.
59. **Zammit PS, Golding JP, Nagata Y, Hudon V, Partridge TA, Beauchamp JR.** 2004. Muscle satellite cells adopt divergent fates: a mechanism for self-renewal? J. Cell Biol. **166**:347–357. http://dx.doi.org/10.1083/jcb.200312007.

Biochemical and Biophysical Research Communications 443 (2014) 917–923

Contents lists available at ScienceDirect

Biochemical and Biophysical Research Communications

journal homepage: www.elsevier.com/locate/ybbrc

The PDZ-binding motif of Yes-associated protein is required for its co-activation of TEAD-mediated *CTGF* transcription and oncogenic cell transforming activity

Tadanori Shimomura, Norio Miyamura, Shoji Hata, Ryota Miura, Jun Hirayama *, Hiroshi Nishina *

Department of Developmental and Regenerative Biology, Medical Research Institute, Tokyo Medical and Dental University, 1-5-45 Yushima, Bunkyo-ku, Tokyo 113-8510, Japan

ARTICLE INFO

Article history:
Received 11 December 2013
Available online 28 December 2013

Keywords:
YAP
Hippo pathway
CTGF
TEAD

ABSTRACT

YAP is a transcriptional co-activator that acts downstream of the Hippo signaling pathway and regulates multiple cellular processes, including proliferation. Hippo pathway-dependent phosphorylation of YAP negatively regulates its function. Conversely, attenuation of Hippo-mediated phosphorylation of YAP increases its ability to stimulate proliferation and eventually induces oncogenic transformation. The C-terminus of YAP contains a highly conserved PDZ-binding motif that regulates YAP's functions in multiple ways. However, to date, the importance of the PDZ-binding motif to the oncogenic cell transforming activity of YAP has not been determined. In this study, we disrupted the PDZ-binding motif in the YAP (5SA) protein, in which the sites normally targeted by Hippo pathway-dependent phosphorylation are mutated. We found that loss of the PDZ-binding motif significantly inhibited the oncogenic transformation of cultured cells induced by YAP (5SA). In addition, the increased nuclear localization of YAP (5SA) and its enhanced activation of TEAD-dependent transcription of the cell proliferation gene *CTGF* were strongly reduced when the PDZ-binding motif was deleted. Similarly, in mouse liver, deletion of the PDZ-binding motif suppressed nuclear localization of YAP (5SA) and YAP (5SA)-induced *CTGF* expression. Taken together, our results indicate that the PDZ-binding motif of YAP is critical for YAP-mediated oncogenesis, and that this effect is mediated by YAP's co-activation of TEAD-mediated *CTGF* transcription.

1. Introduction

The Yes-associated protein (YAP) is a transcriptional co-activator that regulates multiple cellular processes by activating several transcription factors [1]. Recently, YAP was shown to play an important role in organ size control and to be inhibited by the Hippo signaling pathway [2–4]. In mouse liver, either transgenic overexpression of YAP or knock-out of Hippo pathway genes causes enlargement of this organ and the eventual development of hepatic tumors [5,6]. In cultured cells, YAP overexpression promotes proliferation and induces oncogenic transformation by activating TEAD-mediated transcription of the cell proliferation gene connective tissue growth factor (*CTGF*) [7,8]. Thus, the proper control of YAP activity is critical for maintaining tissue homeostasis in animals.

YAP functions are regulated by multiple post-translational modifications, including phosphorylation, SUMOylation, acetylation, and methylation [9–13]. Among these, phosphorylation is the best characterized regulatory event. For example, cell–cell contact triggers the Hippo pathway to phosphorylate YAP and thereby inactivate it, inhibiting cell proliferation. This phosphorylation is mediated by Lats kinases, which are essential components of the Hippo pathway. Lats-mediated phosphorylation of serine 127 (Ser-127) of human YAP (hYAP) promotes its recognition and cytoplasmic retention by 14-3-3 protein [9], while phosphorylation of hYAP Ser-381 induces hYAP ubiquitination and degradation [10]. Thus, the Hippo pathway negatively regulates the transcriptional co-activation capacity of YAP by inducing its cytoplasmic localization and protein degradation.

YAP contains a highly conserved PDZ-binding motif in its C-terminal domain, and this motif reportedly contributes to the regulation of YAP's functions. For example, Oka et al. showed that the interaction of the tight junction protein zonula occludens 2 (ZO2) with YAP's PDZ-binding motif facilitates nuclear localization of YAP [14]. In another study, it was reported that YAP stabilizes p73 to promote apoptosis, and that YAP's PDZ-binding motif is required for this proapoptotic function [15]. Although these studies

Abbreviations: YAP, Yes-associated protein; CTGF, connective tissue growth factor; TEAD, TEA domain family member; TAZ, transcriptional co-activator with PDZ-binding motif.

* Corresponding authors. Fax: +81 3 5803 5829.
E-mail addresses: hirayama.dbio@mri.tmd.ac.jp (J. Hirayama), nishina.dbio@mri.tmd.ac.jp (H. Nishina).

0006-291X/$ - see front matter © 2013 Elsevier Inc. All rights reserved.
http://dx.doi.org/10.1016/j.bbrc.2013.12.100

demonstrate that the PDZ-binding motif is important for regulating YAP's normal functions, the role of this motif in controlling the oncogenic cell transforming activity of YAP has not been characterized.

In this study, we investigated whether the PDZ-binding motif of hYAP is involved in its ability to transform cultured cells using the hYAP (5SA) mutant, which is not under the negative control of the Hippo pathway due to mutation of key phosphorylation sites [9]. As a result, hYAP (5SA) is constitutively activated and abnormally increased in a cell's nucleus. YAP co-transcriptional activity is thus elevated, inducing the oncogenic transformation of cultured cells. We found that disruption of the PDZ-binding motif strongly inhibited these properties of hYAP (5SA) both in cultured cells and mouse liver. Our results thus provide several lines of evidence indicating that the PDZ-binding motif is involved in regulating the nuclear localization of YAP and its co-activator function. In particular, we show that loss of this motif reduces TEAD-mediated transcription of *CTGF*, damping down YAP's oncogenic transforming activity.

2. Materials and methods

2.1. Plasmids

The mouse *CTGF* gene promoter was amplified by PCR and cloned into the pGL3-Basic vector (Promega). The *CTGF* promoter region spans codons −708 to −220 (+1 is the start codon) and contains the TEAD-binding element. Mutations were introduced into Myc-hYAP/pCS2 using PCR-based site-directed mutagenesis to generate mutant forms of hYAP described in each Figure. To inactivate the PDZ-binding motif, the *hYap* cDNA sequences corresponding to the last five amino acids of the hYAP protein were deleted. Other plasmids used in this study have been described elsewhere [12].

2.2. Cells, transfection, and luciferase assay

293T and NIH3T3 cells were grown in Dulbecco's modified Eagle's medium (Invitrogen) supplemented with 10% fetal bovine serum. For luciferase reporter assays, 293T cells were transfected with 40 ng firefly luciferase reporter plasmid, 20 ng sea pansy luciferase reporter plasmid [pRL-SV40 (Promega)], and the appropriate expression plasmids (indicated in each Figure) using Fugene HD (Promega). At 24 h post-transfection, cell lysates were prepared and dual luciferase assays performed using the dual-luciferase reporter assay system (Promega). Firefly and sea pansy luciferase activities were quantified by means of a luminometer, with the firefly luciferase activity normalized for transfection efficiency based on the sea pansy luciferase activity.

2.3. Antibodies

Anti-Myc, anti-lamin A/C, and anti-actin antibodies were purchased from Santa Cruz; rat anti-HA antibody from Roche Diagnostics Corp.; rabbit anti-HA antibody from Immunology Consultants Laboratory; and anti-β-tubulin antibody from Cell Signaling Technology.

2.4. Co-immunoprecipitation

Co-immunoprecipitation was performed as previously described [16], with some modifications. 293T cells were transfected with the expression plasmids described in each Figure. Transfected cells were washed with phosphate-buffered saline, homogenized in binding buffer (150 mM NaCl, 1 mM EDTA, 0.5% Nonidet P-40, 5% glycerol and 20 mM Tris–HCl, pH 7.4) containing protease inhibitor, and clarified by centrifugation. Total protein from the supernatant was incubated at 4 °C with rabbit anti-HA antibody and 20 μl protein G-Sepharose beads. The beads were washed four times with binding buffer, boiled in SDS sample buffer. The supernatant was fractionated by SDS–PAGE and analyzed by Western blotting as described below.

2.5. Western blotting

Immunoprecipitated materials and total cell extracts obtained as described above were fractionated by SDS–PAGE and transferred electrophoretically onto polyvinylidene difluoride membranes. Membranes were blocked with Blocking One (Nacalai Tesque) or 2% skim milk and incubated for 10 h at 4 °C with the antibodies indicated in each Figure. The blots were then incubated with the appropriate secondary antibodies plus peroxidase-conjugated anti-mouse, anti-rabbit, anti-rat, or anti-goat IgG antibodies (Santa Cruz) and developed with the ECL Western blotting detection system (Amersham Biosciences).

2.6. Immunofluorescence

Frozen sections of mouse liver were attached to APS-coated glass slides (Matsunami Glass). After blocking with 5% BSA in TBS, the slides were incubated with primary antibodies followed by fluorescent tag-conjugated secondary antibodies. Nuclei and plasma membranes were counterstained with Hoechst 33342 or phalloidin (both from Invitrogen), respectively.

2.7. Quantitation of nuclear protein in cultured cells

Levels of YAP localized in cellular nuclei were calculated as follows. The signal intensities of bands of YAP proteins appearing on Western blots were measured using the Quantity One (Bio-Rad) and normalized to the signal intensity of the band representing the nuclear protein laminA/C (value 1). The signal intensities of total hYAPs were normalized for protein loading based on the signal intensity of the band representing actin (value 2). Value 1 was divided by value 2 to obtain the value for nuclear hYAP protein.

2.8. Mice

All mice used in this study were of the C57BL/6J genetic background. All experimental procedures in this study were approved by the Institutional Animal Care and Use Committee of Tokyo Medical and Dental University.

2.9. Plasmid injections into living mice

Manipulated genes were expressed in hepatocytes of living mice by the hydrodynamic tail vein injection (HTVi) system. Briefly, each gene of interest was cloned into the pLIVE vector and suspended in *Trans*IT-EE Hydrodynamic Delivery Solution (Mirus Bio). Plasmids were injected into tail veins of mice.

3. Results

3.1. Deletion of the PDZ-binding motif of hYAP (5SA) abolishes its oncogenic transforming activity

We first compared the effects of transient expression of Myc-tagged plasmids expressing wild type hYAP [hYAP (WT)] or several mutant forms of hYAP in NIH3T3 cells. NIH3T3 cells transfected with hYAP (WT) and cultured for an extended period stopped proliferating when they reached saturation density (Fig. 1A). Similar

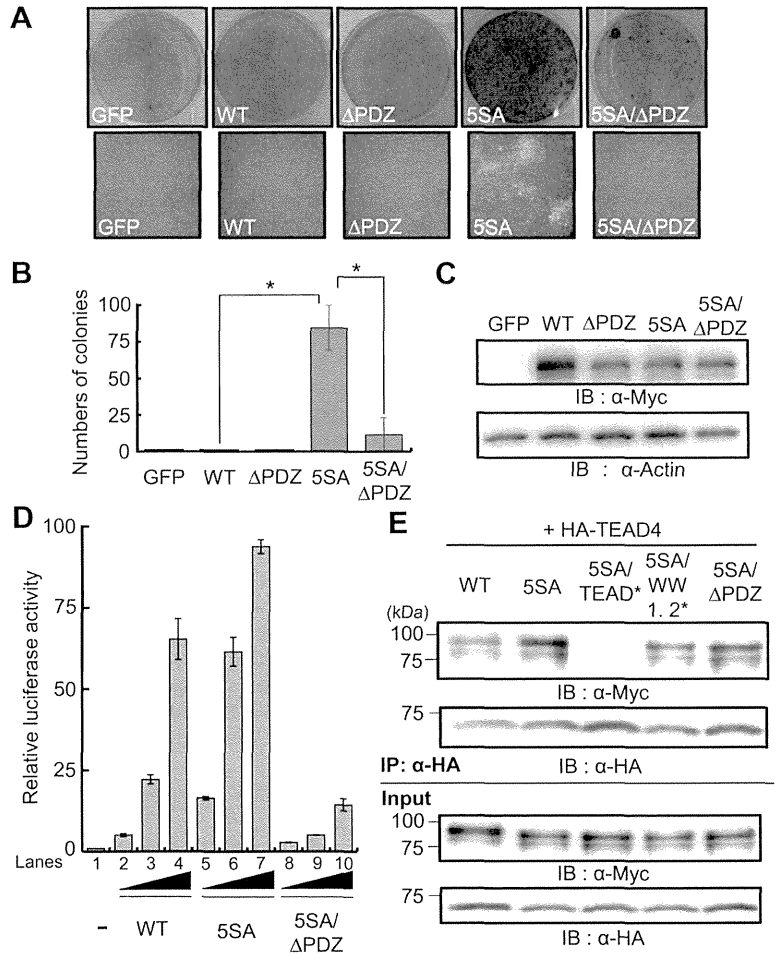

Fig. 1. The PDZ-binding motif of hYAP (5SA) is required for its oncogenic activity. (A) The cell transforming activity of wild type hYAP and various mutant forms of hYAP were determined by colony formation assays. Vectors expressing GFP (control), wild type hYAP (WT), WT hYAP lacking its PDZ-binding motif (ΔPDZ), the hYAP (5SA) mutant (5SA), or the hYAP (5SA) mutant lacking its PDZ-binding motif (5SA/ΔPDZ), were transiently expressed in NIH3T3 cells. At 18 days post-transfection, colonies were visualized by crystal violet staining (upper panels). The corresponding phase-contrast images of these NIH3T3 cells are also shown (lower panels). (B) The numbers of colonies in the plates in (A) were counted. Values are the mean ± S.E. ($n = 3$ plates/group). $^*P < 0.05$. (C) Protein levels of WT hYAP and its mutant forms in the cells in (A) were confirmed by Western blot (WB). (D) Transcriptional co-activation capacities of WT hYAP and its mutant forms were determined by luciferase reporter assays. Wild type hYAP, hYAP (5SA) or hYAP (5SA/ΔPDZ) was co-expressed in 293T cells with TEAD, and transactivation of a luciferase reporter plasmid containing the mouse *CTGF* promoter was examined. Values are the mean ± S.E. ($n = 3$) of luciferase activity relative to that in the sample containing only the reporter plasmid (set to 1). The difference between the results shown in lanes 2 and 5, 3 and 6, 5 and 8, 6 and 9, or 7 and 10 is statistically significant ($P < 0.01$). The difference between the results shown in lanes 4 and 7 is statistically significant ($P < 0.05$). (E) HA-tagged TEAD was co-expressed in 293T cells with Myc-tagged WT hYAP or its mutant forms. Lysates were immunoprecipitated (IP) with anti-HA antibody and analyzed by WB with anti-Myc antibody to detect hYAP proteins, or with anti-HA antibody to detect TEAD. Input: Total cell extracts were analyzed by WB with anti-Myc to detect WT hYAP and its mutant forms, or with anti-HA antibody to detect TEAD. 5SA/TEAD*, hYAP (5SA) with a mutated TEAD-binding domain; 5SA/WW1.2*, hYAP (5SA) with mutated WW domains.

results were observed for cells expressing GFP (control), or hYAP (WT) missing its PDZ-binding motif (hYAP-ΔPDZ). However, when NIH3T3 cells were transiently transfected with the hYAP (5SA) mutant, some of these cells re-initiated proliferation after confluence was reached. Nodules were formed in which the cells began to pile up, a feature of the oncogenic transformation phenotype (Fig. 1A–C). These findings are consistent with a previous report [10] and confirm that Hippo pathway-dependent suppression of hYAP activity inhibits its ability to transform cells. Strikingly, the oncogenic transforming activity of hYAP (5SA) was significantly reduced by deletion of its PDZ-binding motif [hYAP (5SA/ΔPDZ)] (Fig. 1A and B), suggesting that this motif plays an important role in the cell transforming activity of hYAP (5SA).

Previous work has demonstrated that YAP-dependent co-activation of TEAD-mediated transcription of the cell proliferation gene *CTGF* is an important step in the oncogenic cell transformation induced by hYAP (5SA) [7]. We then used a luciferase reporter assay to test whether the PDZ-binding motif of hYAP (5SA) could drive TEAD-mediated transcription from the *CTGF* promoter. As reported elsewhere [9], co-expression of hYAP (WT) enhanced TEAD-mediated *CTGF* transcription in a dose-dependent manner (Fig. 1D). As expected, *CTGF* transcription was significantly increased above this enhanced level when hYAP (5SA) was co-expressed. In contrast, the co-transcriptional activity of co-expressed hYAP (5SA/ΔPDZ) was markedly diminished, indicating that deletion of the PDZ-binding motif impairs the ability of hYAP (5SA) to co-activate TEAD-mediated *CTGF* transcription.

One explanation for our observations could be that deletion of hYAP (5SA)'s PDZ-binding motif affected its interaction with TEAD. To test this possibility, we used co-immunoprecipitation to examine the ability of WT and mutant forms of hYAP to interact with TEAD. HA-TEAD was co-expressed in cultured cells with Myc-hYAP (WT), Myc-hYAP (5SA), Myc-hYAP (5SA/WW1. 2*), or Myc-hYAP (5SA/ΔPDZ), all of which possess an intact TEAD-binding domain.

When cell lysates were subjected to immunoprecipitation with anti-HA antibody, we found that all four forms of hYAP successfully co-immunoprecipitated with HA-TEAD (Fig. 1E). In contrast, hYAP (5SA) bearing a mutated TEAD-binding domain (5SA/TEAD*; negative control) [8] did not co-immunoprecipitate with HA-TEAD. Because hYAP (5SA/ΔPDZ) maintained its TEAD-binding ability, we concluded that the reduced co-transcriptional capacity of hYAP (5SA/ΔPDZ) is not due to an inability to interact with TEAD.

3.2. Deletion of the PDZ-binding motif induces the cytoplasmic localization of hYAP (5SA)

We next tested the effect of PDZ-binding motif deletion on the subcellular localization of hYAP (5SA). Myc-hYAP (WT), Myc-hYAP (5SA) or Myc-hYAP (5SA/ΔPDZ) was expressed in cultured cells and hYAP sub-cellular localization was determined by cell fractionation and Western blotting. hYAP (WT) was detected in both the nucleus and cytoplasm (Fig. 2). Nuclear localization of hYAP (5SA) was significantly increased compared to that of hYAP (WT). These results are consistent with previous reports showing that Hippo-mediated YAP phosphorylation is necessary for its cytoplasmic retention [5,9]. Importantly, compared to Myc-hYAP (5SA), a higher concentration of Myc-hYAP (5SA/ΔPDZ) was present in the cytoplasm than in the nucleus (Fig. 2). Thus, deletion of the PDZ-binding motif blocks the nuclear localization of hYAP (5SA), an event that would account for its impaired promotion of TEAD-mediated *CTGF* transcription.

3.3. Addition of NLS does not rescue nuclear localization of hYAP (ΔPDZ)

To examine whether the addition of a nuclear localization sequence (NLS) to hYAP (ΔPDZ) could restore its nuclear localization, we generated a series of constructs in which the SV40 NLS sequence was inserted into the N-terminus of hYAP (WT) or hYAP (ΔPDZ). The subcellular localization of each of these NLS-fused hYAP proteins was then determined after transfection into 293T cells. We found that the addition of SV40 NLS significantly increased the nuclear localization of hYAP (WT) (Fig. 3A and B), indicating that the NLS was indeed functional. However, NLS addition did not increase the nuclear localization of hYAP (ΔPDZ) (Fig. 3A and B). We also investigated whether NLS fusion altered the co-transcriptional activity of hYAPs during TEAD-mediated *CTGF* transcription. As expected, the activity of NLS-fused hYAP (WT) was significantly greater than that of hYAP (WT) (Fig. 3C). On the other hand, the addition of SV40 NLS had no effect on the already limited co-transcriptional activity of hYAP (ΔPDZ). These results indicate that NLS-dependent nuclear import is insufficient to compensate for the defect in hYAP nuclear localization imposed by loss of its PDZ-binding motif.

3.4. Deletion of the PDZ-binding motif suppresses hYAP (5SA)-mediated co-activation of CTGF transcription in mouse liver

To determine if our results in cultured cells could be extended to the tissues of living mice, we used HTVi to test the effect of

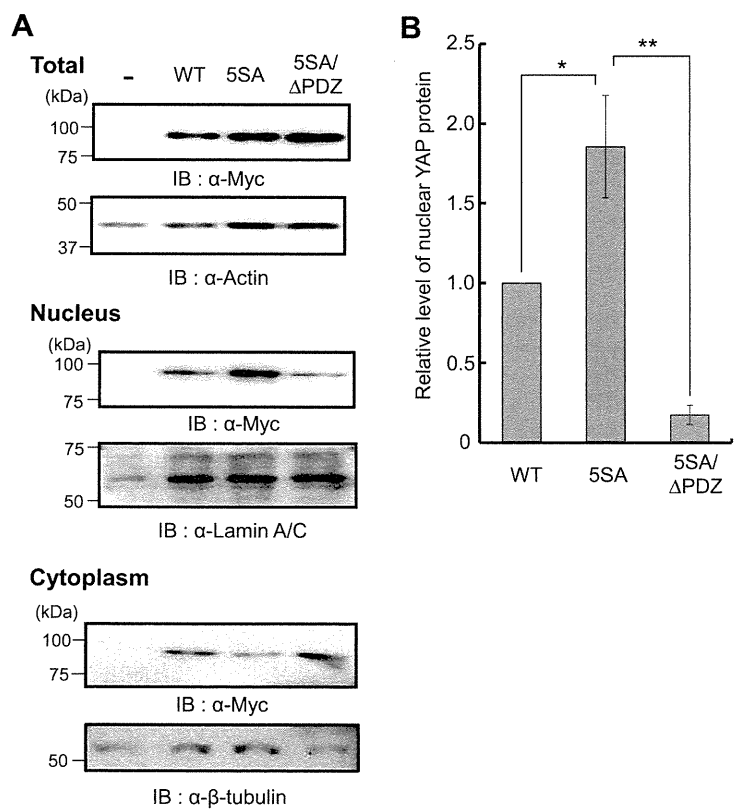

Fig. 2. The PDZ-binding motif of hYAP (5SA) is required for its nuclear localization in cultured cells. (A) Vectors expressing Myc-tagged hYAP (WT), hYAP (5SA), or hYAP (5SA/ΔPDZ) were individually transfected into 293T cells. Lysates were prepared, with some set aside (Total) and the rest subjected to subcellular fractionation to generate cytoplasmic and nuclear fractions. In each case, protein levels of Myc-tagged hYAP (WT) and the indicated mutant hYAP forms were determined by WB with anti-Myc antibody. The presence of the cytoplasmic marker β-tubulin and the nuclear marker lamin A/C in the appropriate fractions was confirmed by WB with the corresponding antibodies. Results shown are representative of three experiments. (B) Quantitative analysis of the nuclear localization of WT hYAP and its mutant forms in the cells in (A). The signal intensities in each lane of the "Nucleus" panel of (A) were measured as described in Section 2. Data are expressed relative to the value of the hYAP (WT) sample (set to 1). Values are the mean ± S.E. ($n = 3$). $^*P < 0.05$, $^{**}P < 0.01$.

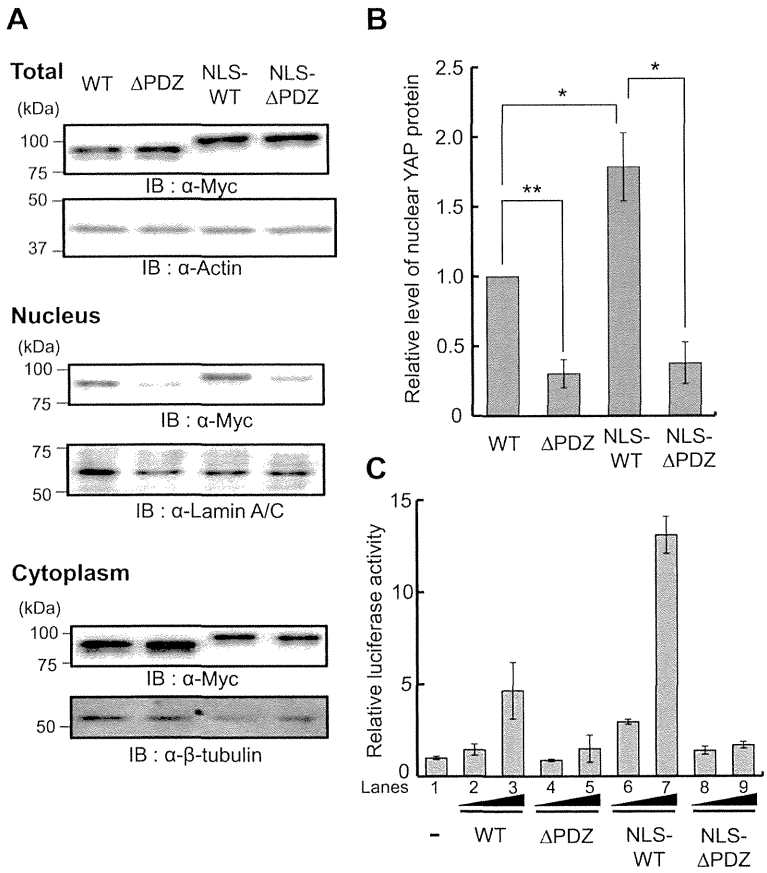

Fig. 3. The SV40 NLS has no effect on the cytoplasmic localization of hYAP (ΔPDZ). (A) Vectors expressing Myc-tagged hYAP (WT), hYAP (ΔPDZ), NLS-fused hYAP (WT), or NLS-fused YAP (ΔPDZ) were individually transfected into 293T cells and subcellular fractionation and analysis were performed as for Fig. 2A. (B) Quantitative analysis of the nuclear localization of hYAP (WT) and the indicated mutant hYAP forms was performed as for Fig. 2B. $^{*}P < 0.05$,$^{**}P < 0.01$. (C) The transcriptional co-activation capacities of hYAP (WT) and the indicated mutant forms were determined by luciferase reporter assay as for Fig. 1D. The difference between the results shown in lanes 7 and 9 is statistically significant ($P < 0.01$). The difference between the results shown in lanes 2 and 6, 3 and 7, or 6 and 8 is statistically significant ($P < 0.05$).

PDZ-binding motif deletion on YAP's subcellular localization in mouse liver. This system results in the safe and efficient delivery of naked nucleic acids to the liver of living mice. Myc-tagged plasmids expressing hYAP (WT), hYAP (5SA) or hYAP (5SA/ΔPDZ) were introduced into mouse liver by HTVi, and nuclear or cytoplasmic localization of each hYAP form was determined by immunofluorescence. When exogenously expressed in mouse liver, Myc-hYAP (WT) was almost exclusively localized in the cytoplasm (Fig. 4A and B). In contrast, Myc-hYAP (5SA) was concentrated in the nucleus and gave only a weak diffuse signal in the cytoplasm. These results confirm that, as in cultured cells, the Hippo pathway regulates YAP subcellular localization in mouse liver. Importantly, hYAP (5SA/ΔPDZ) was mainly located in the cytoplasm, replicating our earlier findings and showing that the PDZ-binding motif of hYAP is crucial for YAP nuclear localization *in vivo*.

We then examined expression levels of *CTGF* in livers of mice that had received HTVi introduction of hYAP (WT) or its mutant forms. As shown in Fig. 4C, levels of *CTGF* mRNA in mouse liver expressing exogenous hYAP (5SA) were much higher than in mouse liver expressing exogenous hYAP (WT). Once again, deletion of the PDZ-binding motif abolished the induction of *CTGF* expression by hYAP (5SA). Taken together, our results clearly demonstrate that the PDZ-binding motif of YAP is required for YAP's nuclear translocation *in vivo* and thus its ability to co-activate *CTGF* transcription.

4. Discussion

YAP can act as an oncoprotein that promotes excessive cell proliferation and induces tumorigenic transformation in both *in vitro* and *in vivo* systems [5,7,17]. It is known that the TEAD family of transcription factors plays an essential role in this YAP-induced proliferation and oncogenic transformation [8]. YAP activates TEAD-mediated transcription of *CTGF*, a cell proliferation gene, which triggers cell growth and eventually oncogenic transformation. Thus, in studies of the constitutively active YAP (5SA) mutant, disruption of either its TEAD-binding domain or transactivation domain suppresses tumorigenic cell transformation [8,9]. We have shown here that the PDZ-binding motif is also required for YAP's oncogenic cell transforming activity (Fig. 1A–C). Deletion of the PDZ-binding motif inhibited the nuclear translocation of hYAP (5SA), reducing its ability to co-activate TEAD-mediated transcription in the nucleus (Fig. 1D, Fig. 2). In addition, *CTGF* expression was significantly decreased in cells expressing hYAP (5SA/ΔPDZ) compared with cells expressing hYAP (5SA) *in vivo* (Fig. 4). Our results therefore imply that dysfunction of the PDZ-binding motif disrupts YAP/TEAD-dependent transcription of the *CTGF* gene in the nucleus, suppressing hYAP (5SA)-induced oncogenic transformation.

Previous studies have established that Hippo-mediated phosphorylation of hYAP promotes its recognition by 14-3-3 protein

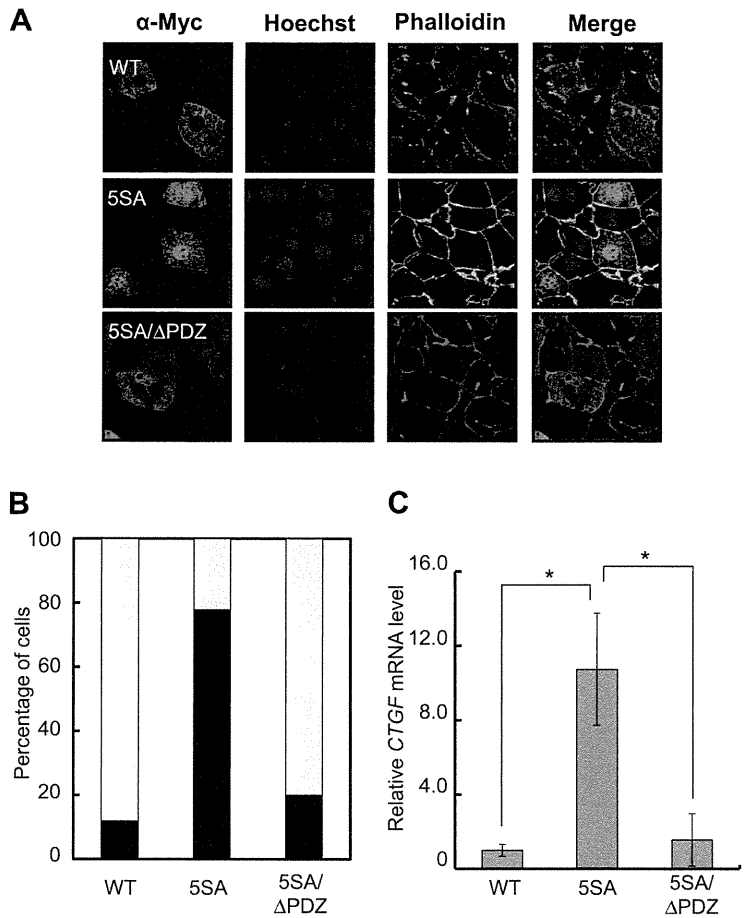

Fig. 4. The PDZ-binding motif is important for the nuclear localization and transcriptional co-activation capacity of hYAP (5SA) in mouse liver. (A) Vectors expressing Myc-tagged hYAP (WT), hYAP (5SA), or hYAP (5SA/ΔPDZ) were individually introduced into mouse liver by HTVi (see Section 2). Myc-tagged hYAPs were detected by staining with anti-Myc followed by fluorescein-conjugated secondary antibody (red). Nuclei and plasma membranes were counterstained with Hoechst 33342 (blue) or phalloidin (green), respectively. (B) Quantitative analysis of the subcellular localization of the exogenous hYAP proteins in (A). For each experimental group, 50–60 cells were evaluated to determine if the fluorescent hYAP protein was predominantly nuclear (black bars) or cytoplasmic (white bars) in localization. Data shown are the percentage of cells showing nuclear vs. cytoplasmic hYAP. (C) Extracts of livers from the mice in (A) were examined by RT-PCR analysis to detect *CTGF* mRNA levels. Data were normalized to expression of mouse *Gapdh* mRNA and are expressed relative to the value of the hYAP (WT) sample (set to 1). Results shown are the mean ± SEM ($n = 3$). $^*P < 0.05$. (For interpretation of the references to color in this figure legend, the reader is referred to the web version of this article.)

and consequently its cytoplasmic retention [9]. We found that deletion of the PDZ-binding motif induced cytoplasmic localization of hYAP (5SA) (Fig. 2 and Fig. 4), suggesting that PDZ-binding motif-dependent nuclear localization of YAP is independent of Hippo-mediated regulation. TAZ is a paralog of YAP, and deletion of the PDZ-binding motif of TAZ inhibits its nuclear localization induced by disruption of Lats-mediated phosphorylation [18]. It is possible that the same subcellular localization control mechanisms operate for both TAZ and YAP.

It has been reported both that the tight junction protein ZO2 binds to YAP's PDZ-binding motif, facilitating YAP's nuclear localization, and that the NLS of ZO2 is required for the ZO2-mediated nuclear localization of YAP [14]. Our results indicate that this NLS-mediated mechanism is insufficient for PDZ-binding motif-dependent nuclear translocation of YAP (Fig. 3). Conceivably, ZO2 binding to YAP's PDZ-binding motif mediates the interaction of YAP with the other factor(s) promoting nuclear localization, or induces a conformational change in YAP that promotes its nuclear translocation. The identification of novel proteins interacting with the PDZ-binding motif of YAP and the delineation of their roles in the control of YAP activity will lead to a clearer understanding of YAP's biological functions.

Acknowledgments

This work was supported in part by research Grants from the Ministry of Education, Culture, Sports, Science and Technology of Japan (J.H. and H.N.), and from the Ministry of Health, Labour and Welfare of Japan (H.N.).

References

[1] R. Yagi, L.F. Chen, K. Shigesada, Y. Murakami, Y. Ito, A WW domain-containing yes-associated protein (YAP) is a novel transcriptional co-activator, EMBO J. 18 (1999) 2551–2562.
[2] G. Halder, R.L. Johnson, Hippo signaling: growth control and beyond, Development 138 (2011) 9–22.
[3] A. Genevet, N. Tapon, The Hippo pathway and apico-basal cell polarity, Biochem. J. 436 (2011) 213–224.
[4] B. Zhao, K. Tumaneng, K.L. Guan, The Hippo pathway in organ size control, tissue regeneration and stem cell self-renewal, Nat. Cell Biol. 13 (2011) 877–883.
[5] J. Dong, G. Feldmann, J. Huang, S. Wu, N. Zhang, S.A. Comerford, M.F. Gayyed, R.A. Anders, A. Maitra, D. Pan, Elucidation of a universal size-control mechanism in Drosophila and mammals, Cell 130 (2007) 1120–1133.
[6] D. Zhou, C. Conrad, F. Xia, J.S. Park, B. Payer, Y. Yin, G.Y. Lauwers, W. Thasler, J.T. Lee, J. Avruch, N. Bardeesy, Mst1 and Mst2 maintain hepatocyte quiescence and suppress hepatocellular carcinoma development through inactivation of the Yap1 oncogene, Cancer Cell 16 (2009) 425–438.

[7] M. Overholtzer, J. Zhang, G.A. Smolen, B. Muir, W. Li, D.C. Sgroi, C.X. Deng, J.S. Brugge, D.A. Haber, Transforming properties of YAP, a candidate oncogene on the chromosome 11q22 amplicon, Proc. Natl. Acad. Sci. USA 103 (2006) 12405–12410.

[8] B. Zhao, X. Ye, J. Yu, L. Li, W. Li, S. Li, J.D. Lin, C.Y. Wang, A.M. Chinnaiyan, Z.C. Lai, K.L. Guan, TEAD mediates YAP-dependent gene induction and growth control, Genes Dev. 22 (2008) 1962–1971.

[9] B. Zhao, X. Wei, W. Li, R.S. Udan, Q. Yang, J. Kim, J. Xie, T. Ikenoue, J. Yu, L. Li, P. Zheng, K. Ye, A. Chinnaiyan, G. Halder, Z.C. Lai, K.L. Guan, Inactivation of YAP oncoprotein by the Hippo pathway is involved in cell contact inhibition and tissue growth control, Genes Dev. 21 (2007) 2747–2761.

[10] B. Zhao, L. Li, K. Tumaneng, C.Y. Wang, K.L. Guan, A coordinated phosphorylation by Lats and CK1 regulates YAP stability through SCF(beta-TRCP), Genes Dev. 24 (2010) 72–85.

[11] E. Lapi, S. Di Agostino, S. Donzelli, H. Gal, E. Domany, G. Rechavi, P.P. Pandolfi, D. Givol, S. Strano, X. Lu, G. Blandino, PML, YAP, and p73 are components of a proapoptotic autoregulatory feedback loop, Mol. Cell 32 (2008) 803–814.

[12] S. Hata, J. Hirayama, H. Kajiho, K. Nakagawa, Y. Hata, T. Katada, M. Furutani-Seiki, H. Nishina, A novel acetylation cycle of transcription co-activator Yes-associated protein that is downstream of Hippo pathway is triggered in response to SN2 alkylating agents, J. Biol. Chem. 287 (2012) 22089–22098.

[13] M.J. Oudhoff, S.A. Freeman, A.L. Couzens, F. Antignano, E. Kuznetsova, P.H. Min, J.P. Northrop, B. Lehnertz, D. Barsyte-Lovejoy, M. Vedadi, C.H. Arrowsmith, H. Nishina, M.R. Gold, F.M. Rossi, A.C. Gingras, C. Zaph, Control of the hippo pathway by Set7-dependent methylation of Yap, Dev. Cell 26 (2013) 188–194.

[14] T. Oka, E. Remue, K. Meerschaert, B. Vanloo, C. Boucherie, D. Gfeller, G.D. Bader, S.S. Sidhu, J. Vandekerckhove, J. Gettemans, M. Sudol, Functional complexes between YAP2 and ZO-2 are PDZ domain-dependent, and regulate YAP2 nuclear localization and signalling1, Biochem. J. 432 (2010) 461–472.

[15] T. Oka, M. Sudol, Nuclear localization and pro-apoptotic signaling of YAP2 require intact PDZ-binding motif, Genes Cells 14 (2009) 607–615.

[16] Y. Uchida, T. Osaki, T. Yamasaki, T. Shimomura, S. Hata, K. Horikawa, S. Shibata, T. Todo, J. Hirayama, H. Nishina, Involvement of stress kinase mitogen-activated protein kinase kinase 7 in regulation of mammalian circadian clock, J. Biol. Chem. 287 (2012) 8318–8326.

[17] L. Zender, M.S. Spector, W. Xue, P. Flemming, C. Cordon-Cardo, J. Silke, S.T. Fan, J.M. Luk, M. Wigler, G.J. Hannon, D. Mu, R. Lucito, S. Powers, S.W. Lowe, Identification and validation of oncogenes in liver cancer using an integrative oncogenomic approach, Cell 125 (2006) 1253–1267.

[18] F. Kanai, P.A. Marignani, D. Sarbassova, R. Yagi, R.A. Hall, M. Donowitz, A. Hisaminato, T. Fujiwara, Y. Ito, L.C. Cantley, M.B. Yaffe, TAZ: a novel transcriptional co-activator regulated by interactions with 14-3-3 and PDZ domain proteins, EMBO J. 19 (2000) 6778–6791.

The Hippo Pathway Controls a Switch between Retinal Progenitor Cell Proliferation and Photoreceptor Cell Differentiation in Zebrafish

Yoichi Asaoka[1]*, Shoji Hata[1], Misako Namae[1], Makoto Furutani-Seiki[2], Hiroshi Nishina[1]*

1 Department of Developmental and Regenerative Biology, Medical Research Institute, Tokyo Medical and Dental University, Tokyo, Japan, **2** Centre for Regenerative Medicine, Department of Biology and Biochemistry, University of Bath, Claverton Down, Bath, United Kingdom

Abstract

The precise regulation of numbers and types of neurons through control of cell cycle exit and terminal differentiation is an essential aspect of neurogenesis. The Hippo signaling pathway has recently been identified as playing a crucial role in promoting cell cycle exit and terminal differentiation in multiple types of stem cells, including in retinal progenitor cells. When Hippo signaling is activated, the core Mst1/2 kinases activate the Lats1/2 kinases, which in turn phosphorylate and inhibit the transcriptional cofactor Yap. During mouse retinogenesis, overexpression of Yap prolongs progenitor cell proliferation, whereas inhibition of Yap decreases this proliferation and promotes retinal cell differentiation. However, to date, it remains unknown how the Hippo pathway affects the differentiation of distinct neuronal cell types such as photoreceptor cells. In this study, we investigated whether Hippo signaling regulates retinogenesis during early zebrafish development. Knockdown of zebrafish *mst2* induced early embryonic defects, including altered retinal pigmentation and morphogenesis. Similar abnormal retinal phenotypes were observed in zebrafish embryos injected with a constitutively active form of *yap* [*(yap (5SA)*]. Loss of Yap's TEAD-binding domain, two WW domains, or transcription activation domain attenuated the retinal abnormalities induced by *yap (5SA)*, indicating that all of these domains contribute to normal retinal development. Remarkably, *yap (5SA)*-expressing zebrafish embryos displayed decreased expression of transcription factors such as *otx5* and *crx*, which orchestrate photoreceptor cell differentiation by activating the expression of *rhodopsin* and other photoreceptor cell genes. Co-immunoprecipitation experiments revealed that Rx1 is a novel interacting partner of Yap that regulates photoreceptor cell differentiation. Our results suggest that Yap suppresses the differentiation of photoreceptor cells from retinal progenitor cells by repressing Rx1-mediated transactivation of photoreceptor cell genes during zebrafish retinogenesis.

Citation: Asaoka Y, Hata S, Namae M, Furutani-Seiki M, Nishina H (2014) The Hippo Pathway Controls a Switch between Retinal Progenitor Cell Proliferation and Photoreceptor Cell Differentiation in Zebrafish. PLoS ONE 9(5): e97365. doi:10.1371/journal.pone.0097365

Editor: Hiroyasu Nakano, Toho University School of Medicine, Japan

Received January 24, 2014; **Accepted** April 17, 2014; **Published** May 14, 2014

Funding: This work was supported by a Grant-in-Aid for Scientific Research on Innovative Areas from the Ministry of Education, Culture, Sports, Science, and Technology of Japan, a Grant-in-Aid for Scientific Research (C) from the Japan Society for the Promotion of Science, and a Grant-in-Aid from the Ministry of Health, Labor and Welfare of Japan. The funders had no role in study design, data collection and analysis, decision to publish, or preparation of the manuscript.

Competing Interests: The authors have declared that no competing interests exist.

* E-mail: y-asaoka.dbio@mri.tmd.ac.jp (YA); nishina.dbio@mri.tmd.ac.jp (HN)

Introduction

In the vertebrate embryonic nervous system, multipotent neural progenitor cells proliferate and differentiate into diverse neuronal and glial cell types that eventually build up functional neural circuits such as the retina [1,2]. The retina is a delicate multilayered neural epithelium composed of six types of neurons and one major type of glial cell [3]. During the course of retinal development, retinal progenitor cells (RPCs) either continue to proliferate or exit mitosis and differentiate into various neuronal cell types. This process is tightly regulated and ensures that the proper numbers and types of differentiated cells needed to assemble a functional retinal circuitry are produced [1,2]. A fundamental mystery in retinal development has been the identity of the molecular mechanism controlling the developmental switch between RPC self-renewal and differentiation. Although rodent models have provided valuable insights into the molecular basis of vertebrate retinal development [4], the zebrafish (*Danio rerio*) is a good alternative in which to seek the definitive answer to this question [5,6]. Fertilized zebrafish eggs rapidly develop *ex utero* into transparent embryos, facilitating retinal observations and experimental manipulations such as morpholino knockdown and the use of transgenic technology. In addition, aspects of retinal morphogenesis and histology, as well as the molecular components governing retinal development, are highly conserved between zebrafish and mammals.

The FGF, Shh, Wnt and Notch signaling pathways have all been identified as affecting retinal cell proliferation and differentiation [7]. For instance, the Notch pathway normally suppresses photoreceptor cell production in the mammalian retina, whereas inhibition of Notch signaling enhances the expression of the *Otx2* and *Crx* genes, which encode transcription factors (TFs) expressed exclusively in photoreceptor cells [8–10]. Another important pathway recently shown to be involved in regulating the balance between RPC maintenance and differentiation is the Hippo signaling cascade [11]. Hippo signaling plays fundamental roles in organ size control, stem cell maintenance, and progenitor differentiation in a variety of tissues, including the central nervous